Review Article

Cell-Free Integrated Sensing and Communication: Principles, Advances, and Future Directions

Diluka Galappaththige[1], Mohammadali Mohammadi[2], Gayan Aruma Baduge[3], Chintha Tellambura[1]

1. Department of Electrical and Computer Engineering, University of Alberta, Canada; 2. Centre for Wireless Innovation (CWI), Queen's University Belfast, Belfast, United Kingdom; 3. School of Electrical, Computer, and Biomedical Engineering, Northern Illinois University, United States

Cell-free (CF) integrated sensing and communication (ISAC) combines CF architecture with ISAC. CF employs distributed access points, eliminates cell boundaries, and enhances coverage, spectral efficiency, and reliability. ISAC unifies radar sensing and communication, enabling simultaneous data transmission and environmental sensing within shared spectral and hardware resources. CF-ISAC leverages these strengths to improve spectral and energy efficiency while enhancing sensing in wireless networks. As a promising candidate for next-generation wireless systems, CF-ISAC supports robust multi-user communication, distributed multi-static sensing, and seamless resource optimization. However, a comprehensive survey on CF-ISAC has been lacking. This paper fills that gap by first revisiting CF and ISAC principles, covering cooperative transmission, radar cross-section, target parameter estimation, ISAC integration levels, sensing metrics, and applications. It then explores CF-ISAC systems, emphasizing their unique features and the benefits of multi-static sensing. State-of-the-art developments are categorized into performance analysis, resource allocation, security, and user/target-centric designs, offering a thorough literature review and case studies. Finally, the paper identifies key challenges such as synchronization, multi-target detection, interference management, and fronthaul capacity and latency. Emerging trends, including next-generation antenna technologies, network-assisted systems, near-field CF-ISAC, integration with other technologies, and machine learning approaches, are highlighted to outline the future trajectory of CF-ISAC research.

Abbreviations

- 5G – Fifth generation
- 6G – Sixth generation
- AN – Artificial noise
- AO – Alternating optimization
- AoA – Angle of arrival
- AP – Access point
- AWGN – Additive white Gaussian noise
- BCD – Block coordinate descend
- BS – Base station
- CF – Cell-free
- CFMM – Cell-free massive multiple-input multiple-output
- CoMP – Coordinated multi-point
- CPU – Central processing unit
- CRB – Cramér-Rao bound
- CRLB – Cramér-Rao lower bound
- CSI – Channel state information
- DAS – Distributed antenna system

 doi.org/10.32388/8SSIYA

- DL – Downlink
- DoF – Degrees of freedom
- EE – Energy efficiency
- EM – Electromagnetic
- FD – Full-duplex
- GLRT – Generalized likelihood ratio test
- HMIMO – Holographic multiple-input multiple-output
- IoT – Internet of Things
- ISAC – Integrated sensing and communication
- LoS – Line-of-sight
- MI – Mutual information
- MIMO – Multiple-input multiple-output
- ML – Machine learning
- mMIMO – Massive multiple-input multiple-output
- MRC – Maximum ratio combining
- MRT – Maximum ratio transmission
- MSE – Mean-square error
- MUSIC – Multiple signal classification
- NLoS – Non-line-of-sight
- OFDM – Orthogonal frequency division multiplexing
- QoS – Quality-of-service
- RCS – Radar cross-section
- RIS – Reconfigurable intelligent surface
- RSU – Roadside units
- SCA – Successive convex approximation
- SCNR – Signal-to-clutter-plus-noise-ratio
- SDR – Semidefinite relaxation
- SE – Spectral efficiency
- SI – Self-interference
- SIC – Successive interference cancellation
- SINR – Signal-to-interference-plus-noise ratio
- SNR – Signal-to-noise ratio
- UAV – Unmanned aerial vehicle
- UC – User-centric
- UL – Uplink
- ULA – Uniform linear array
- UMi – Urban micro
- URLLC – Ultra-reliable low-latency communication
- V2X – Vehicle-to-everything

I. Introduction

Integrated sensing and communication (ISAC) is poised to become a key component of future wireless standards[1][2][3][4][5]. Sensing enables networks to detect, localize, and track objects or environmental features within their coverage area by utilizing transmitted signals to gather information about targets, such as angle, range, velocity, shape, composition, or orientation[1][2][3][4][5]. The dual functions of communication and sensing can support diverse emerging applications, including the Internet of Things (IoT), vehicle-to-everything (V2X) communications, smart traffic control, virtual/augmented reality, smart homes/cities, unmanned aerial vehicles (UAVs), factory automation, and more[1][2][3][4][5].

ISAC enables communication and sensing to efficiently share infrastructure, hardware, signal processing modules, and scarce spectrum and power resources[1][2][3][4][5]. For example, a base station (BS) with multiple antennas can direct beams toward users for communication while using others to monitor surrounding targets or environmental changes[1][2][3][4][5]. This dual functionality improves resource efficiency, reduces hardware and deployment costs, and facilitates seamless coordination between communication and sensing. Additionally, the BS can leverage sensing to estimate channels by analyzing the reflected signals and optimize communication beamforming[1]. By jointly designing and optimizing sensing and communication tasks, waveforms, beamforming, and resource allocation, co-channel interference can be mitigated, which unlocks new design degrees of freedom (DoF) to enhance overall system performance[1][2][3][4][5].

Most current ISAC studies focus on co-located multiple-input multiple-output (MIMO)/massive MIMO (mMIMO) cellular networks, i.e., one BS serves as an ISAC transceiver using mono-static sensing or two BSs act as the ISAC transmitter and sensing receiver utilizing bi-static sensing[1][2][3][4][5]. However, multiple ISAC BSs will operate in the same geographical region, sharing the frequency and timing resources. Furthermore, mono-static and bi-static ISAC systems can only provide limited service coverage and communication and sensing capabilities. In particular, when there are numerous obstacles in the environment and/or when the communication users and sensing targets are dispersed from the BS[6][7][8][9][10][11][12][13][14]. This causes performance degradation, especially for cell-edge users/targets, frequent cell switching, and severe interference between communications and sensing[6][7][8][9][10][11][12][13][14].

To overcome such challenges, cooperation among multiple ISAC BSs or access points (APs) can improve communication and sensing performance[6][7][8][9][10][11][12][13][14]. On the other hand, recent advances in multi-BS/AP communication cooperation, such as coordinated multi-point (CoMP) transmission/reception, cloud-radio access networks, cell-free (CF) MIMO, distributed MIMO radar sensing, and networked ISAC, lay the groundwork for addressing the aforementioned challenges in conventional ISAC systems[15][16][17][18][19][20]. This ultimately leads to CF-ISAC systems, in which distributed ISAC APs jointly serve the same set of communication users and detect the same targets employing multi-static sensing[6][7][8][9][10][11][12][13][14]. Multi-static sensing involves multiple spatially distributed transmitters and receivers to detect and track targets/objects, improving detection, localization, and tracking accuracy[21]. However, it faces challenges such as synchronization, complex signal processing, and deployment costs. In CF-ISAC networks, multi-static sensing can offer a diversity gain by utilizing multiple uncorrelated sensing observations at distributed sensing receivers. Also, multi-static sensing can improve performance by increasing joint transmit/receive beamforming gain through the use of many transmitters/receivers in the network[6][7][8][9][10][11][12][13][14].

A. Existing Survey Papers and Contribution

While CF-ISAC has attracted significant research attention, no survey papers exist. In contrast, separate surveys and tutorials exist for CF communication[22][23][24][25][26][27][28][29][30] and co-located ISAC systems[1][2][3][4][5]. This study decisively addresses this critical gap by reviewing CF-ISAC advancements in-depth, uncovering its capabilities, tackling challenges, and charting future directions for this technology (Fig. 1).

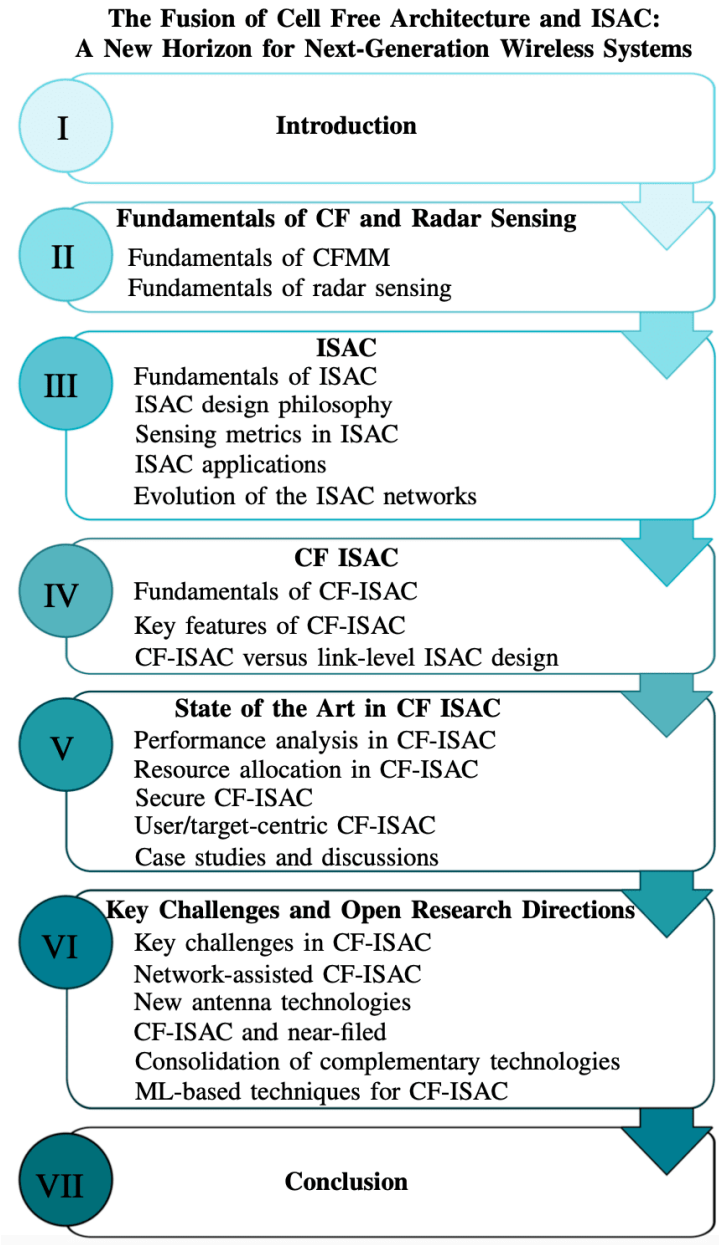

Figure 1. Outline of the main contributions of this paper.

The contributions of this survey paper are summarized as follows:

1. A comprehensive discussion of CF-ISAC systems requires an examination of the core principles of CF-mMIMO (CFMM) and sensing. The discussion begins with an overview of CFMM, including cooperative transmission and reception, channel hardening, favorable propagation, and key performance metrics. Next, sensing fundamentals are explored, covering radar cross-section (RCS), clutter, signal transmission, radar types, sensing techniques, and methods for estimating target parameters.
2. To establish the fundamentals of CF-ISAC networks, conventional ISAC systems and their properties are examined. Specifically, the discussion covers the levels of integration in ISAC systems, ISAC design philosophies, sensing metrics, and ISAC applications.

3. With the foundational concepts established, the focus shifts to CF-ISAC systems and their unique characteristics. An in-depth analysis highlights the advantages of multi-static sensing in CF-ISAC over conventional ISAC, emphasizing its superior sensing capabilities. Key features are examined in detail, including distributed antenna systems (DAS), seamless handovers, user- and target-centric operations, advanced interference management, efficient resource allocation, AP cooperation, and robust synchronization mechanisms.
4. State-of-the-art, CF-ISAC technical contributions are categorized into four key areas: performance analysis, resource allocation, secure CF-ISAC, and user/target-centric CF-ISAC. A detailed literature review is conducted for each category, highlighting methodologies, studies, and key findings. Additionally, case studies with extensive simulations evaluate CF-ISAC system performance across these areas, offering more profound insights into their operational effectiveness and potential.
5. Finally, the remaining challenges, open issues, and emerging trends in CF-ISAC systems are examined. Key challenges are addressed, including synchronization, multi-target detection, interference management, and fronthaul capacity and latency. Additionally, open research directions and future trends are highlighted, such as advancements in network-assisted CF-ISAC, the development of new antenna technologies, the integration of complementary technologies, and the application of machine learning (ML) techniques. These insights outline potential pathways for further innovation in the field.

This paper is organized as follows: Section II provides an overview of CF architecture and radar sensing fundamentals. Section III covers the basics of conventional ISAC systems and recent advancements. Section IV delves into CF-ISAC systems, highlighting their fundamentals, unique features, and advantages. Section V reviews current technical contributions and presents case studies. Finally, Section VI discusses future research directions, opportunities, and challenges.

Notation: Boldface lower and upper case letters denote vectors and matrices. $\mathbb{C}^{M\times N}$ and $\mathbb{R}^{M\times 1}$ represent $M\times N$ dimensional complex matrices and $M\times 1$ dimensional real vectors, respectively. For a square matrix $\mathbf{A}$, $\mathbf{A}^H$ and $\mathbf{A}^T$ are the Hermitian conjugate transpose and transpose, respectively. $\mathbf{I}_M$ denotes the M-by-M identity matrix. $\mathbf{0}_M$ is the M-dimensional all-zero vector. The Euclidean norm of a complex vector and the absolute value of a complex scalar are denoted by $\|\cdot\|$ and $|\cdot|$, respectively. Expectation, the real part of a complex number, and trace operation are denoted by $\mathbb{E}\{\cdot\}$, $\mathrm{Re}\{\cdot\}$, and $\mathrm{Tr}(\cdot)$, respectively. A circularly symmetric complex Gaussian (CSCG) random vector with mean μ and covariance matrix $\mathbf{C}$ is denoted by $\sim\mathcal{CN}(\mu,\mathbf{C})$. Finally, $[\mathbf{A}]_{ij}$ is the $\{i,j\}$-th element of $\mathbf{A}$.

II. Fundamentals of Cell-Free Architecture and Radar Sensing

This section overviews two key concepts: CF architecture and radar sensing. CF networks enhance coverage, capacity, and user experience by enabling distributed APs to collaboratively serve users without centralized BSs. Radar sensing, a core element of ISAC, provides real-time environmental awareness by detecting and tracking objects using electromagnetic (EM) waves. These technologies underpin this study, offering innovative solutions for future ISAC systems.

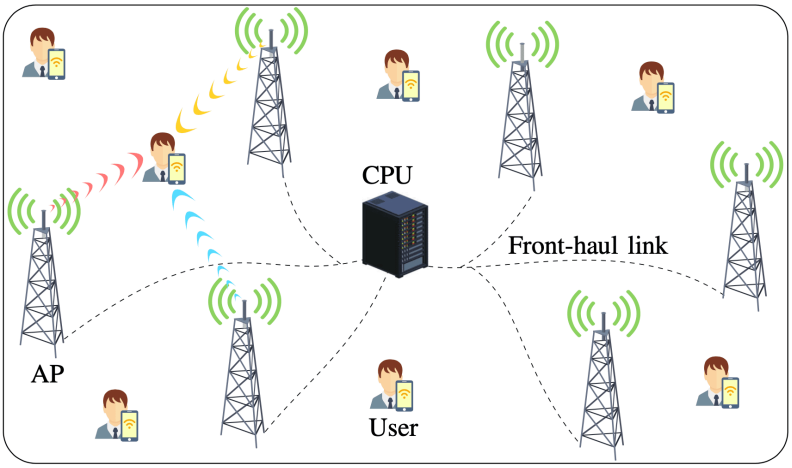

Figure 2. A CFMM system.

A. Fundamentals of Cell-Free Massive MIMO

CFMM is a next-generation wireless communication paradigm that replaces the traditional cellular structure with a seamless, collaborative approach to user connectivity[22][18][27][31][32][33][34][35][36]. In conventional co-located mMIMO, the BS in each cell employs many antennas, typically 64 or more, to serve users within the cell[37][38]. In contrast, CFMM uses a distributed array of APs to collaboratively serve all users within a large geographical area (Fig. 2). This configuration offers advantages over traditional cellular architectures, including improved spectral efficiency (SE), energy efficiency (EE), uniform service quality, and enhanced robustness to interference and shadowing effects[39].

1. Elimination of Cell-Boundaries

The departure from cell-based architectures by deploying APs across a large region without forming discrete cells overcomes the performance limitations of co-located mMIMO. The network is thus treated as a single cohesive unit, where multiple APs simultaneously serve each user, ensuring consistent and uniform service quality regardless of the user's location[22][18][27][31][32][33][34][35][36].

The absence of cell boundaries eliminates the requirement for cell handovers, which frequently cause latency and service outages in traditional cellular systems. Instead, users experience seamless connectivity through cooperative transmission and reception facilitated by the distributed APs[22][18][27][40]. This approach enhances performance by exploiting spatial diversity, as multiple APs serve each user. The APs are closer to the user, reducing the path loss and improving reliability, particularly in challenging propagation environments[22][18][27][40].

Nevertheless, the CF architecture also introduces unique challenges. The distributed nature creates substantial fronthaul signaling for acquiring channel state information (CSI) and data sharing among APs, leading to higher communication overhead. Also, centralized or coordinated processing to handle distributed resources can result in high computational complexity. For instance, the fronthaul capacity, fronthaul signaling, and computational complexity linearly scale (or faster) with the number of APs and users[41][42]. Despite these challenges, CFMM offers substantial benefits over alternatives like DAS and CoMP, where static, disjoint cooperation clusters limit inter-cell collaboration[43][44][45][46]. By dynamically and flexibly coordinating APs across the entire network, CFMM achieves superior performance, especially in high user density and mobility scenarios[22][18][27].

2. Cooperative Transmission and Reception

In CFMM, cooperative transmission and reception involve the collaborative operation of distributed APs to jointly serve users, coordinated by a central processing unit (CPU)[22][18][27]. This cooperation eliminates cell boundaries, enhances signal quality through spatial diversity, reduces interference, and improves SE and EE[22][18][27]. It is necessary to ensure seamless connectivity, uniform service quality, and reliable communication, especially in dynamic and high-density user environments[22][18][27].

1. **CPU Coordination:** The CPU acts as the central intelligence of the CFMM system. It collects globally or locally estimated CSI from all APs to perform centralized beamforming, resource allocation, and other tasks. Unlike conventional cellular systems, where inter-cell interference limits performance, this coordinated framework minimizes interference while maximizing SE and EE and optimizing the network performance (Section II-A4). Key functions of the CPU include:
   - *CSI acquisition:* Each AP locally estimates CSI and forwards it to the CPU. The CUP uses this information to compute accurate multi-user beamforming and manage user-specific scheduling. This ensures that APs collaboratively transmit coherent signals, reducing interference and improving SE[22][18][27].
   - *Centralized processing:* With the acquired CSI, the CPU designs downlink (DL) beamforming weights/vectors for each AP to ensure constructive interference at the users. For the uplink (UL), the CPU performs joint decoding by coherently combining signals received by multiple APs, leveraging macro-diversity[22][18][27].
   - *Dynamic resource allocation:* The CPU can dynamically allocate system resources, such as power, spectrum resources, and user scheduling, based on the real-time requirements of users. This ensures uniform service quality across the network[22][18][27]. Power control algorithms, such as max-min fairness or sum-rate maximization, can also balance SE and EE trade-offs.

However, this centralized coordination requires precise synchronization and fronthaul infrastructure.

2. *Synchronization:* APs must be synchronized to ensure coherent transmission and reception. Specifically, both time and phase synchronization are essential[22][18][27]. Time synchronization refers to aligning the clocks of multiple APs so that their signals arrive at the intended users simultaneously, ensuring precise timing and preventing inter-symbol interference. Phase synchronization involves aligning the phase of signals transmitted from different APs, which is critical for coherent beamforming. In this process, signal phases must be accurately matched to maximize constructive interference at the users, thereby enhancing signal strength and system performance[22][18][27].
3. *Fronthaul:* Cooperative operation requires a robust fronthaul network for real-time data and CSI exchange between APs and the CPU. In dense networks, frequent CSI, user data, and control exchanges generate significant fronthaul traffic. Low-latency, high-bandwidth links, such as fiber or mmWave backhaul, are essential for real-time processing[22][18][27].

   Fronthaul architectures can be broadly categorized into centralized and distributed systems[47]. In centralized architectures (e.g., Cloud-RAN), all baseband processing is handled at a central unit (CPU), simplifying network management but placing higher demands on the fronthaul for bandwidth and latency[48]. In contrast, distributed architectures (e.g., Fog-RAN or Edge-RAN) push some processing closer to the APs, reducing fronthaul load but increasing complexity at the network edge[49].

   Optimizing fronthaul networks involves several strategies:

   1. Compression Techniques: Applying data and CSI compression algorithms can significantly reduce fronthaul traffic while maintaining acceptable performance levels.
   2. Functional Splitting: Dynamically adjusting the division of processing tasks between the APs and the CPU (i.e., functional splits) can balance fronthaul load and processing latency based on network conditions.
   3. Resource Allocation: Efficient scheduling and allocation of fronthaul bandwidth can prioritize critical CSI and user data, reducing latency and congestion.

4. Hybrid Fronthaul Solutions: Combining fiber and wireless (e.g., mmWave or Free Space Optics) links can offer flexibility, cost-efficiency, and redundancy to enhance network resilience.

Furthermore, synchronization protocols across the fronthaul network, such as the Institute of Electrical and Electronics Engineers (IEEE) 1588 Precision Time Protocol (PTP), are critical to ensure the timely and coherent exchange of signals, especially for advanced applications like CoMP and CFMM.

3. Multiple Antenna Effects

When APs use multiple antennas to communicate with distributed user terminals, two critical phenomena arise: Channel hardening and Favorable propagation[22].

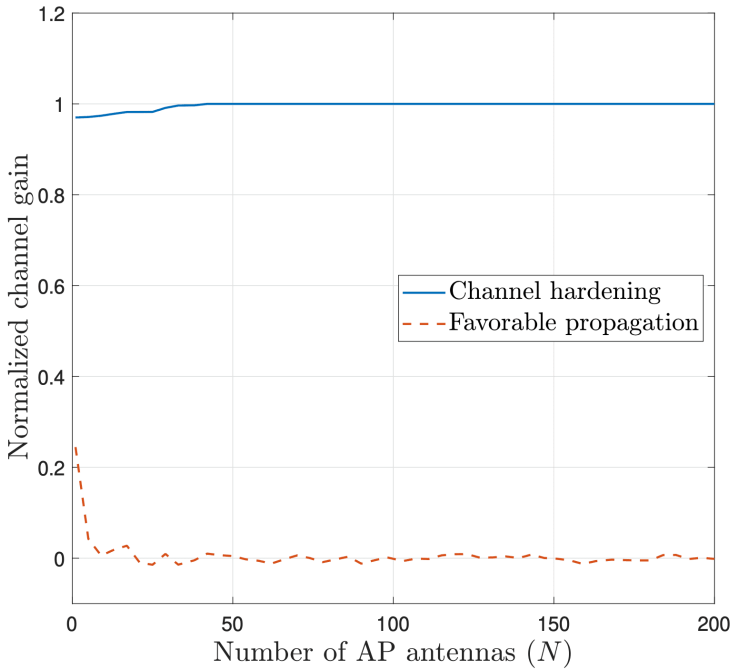

Figure 3. Channel hardening and favorable propagation versus the number of AP antennas, N, assuming i.i.d. Rayleigh fading.

1. **Channel Hardening:** This refers to the diminishing effect of small-scale fading as the number of AP antennas increases. Thus, the channel tends to a deterministic gain with reduced variability, resulting in negligible fluctuations around the channel's mean[22][50] [27][51]. To illustrate, let's denote the channel between the m-th AP with N antennas and the k-th single-antenna user as $\mathbf{h}_{mk} = [h_{mk,1}, \ldots, h_{mk,N}]^T \in \mathbb{C}^{N\times 1}$, where $h_{mk,n}$ is the channel gain between the n-th antenna element and the user. For simplicity, $h_{mk,n}$'s are assumed independent and identically distributed (i.i.d.) Rayleigh fading coefficients, i.e., $h_{mk,n} \sim \mathcal{CN}(0, \beta_{mk})$, where β_{mk} accounts for the large-scale path-loss and shadowing. Then, the coefficient of variation of the instantaneous channel gain, i.e., $\|\mathbf{h}_{mk}\|^2$, which is a measure of the variability relative to the mean, is given as[22]

$$CV = \frac{\|\mathbf{h}_{mk}\|^2}{\mathbb{E}\left\{\|\mathbf{h}_{mk}\|^2\right\}} \to 1 \quad \text{as} \quad N \to \infty. \tag{1}$$

As $N \to \infty$, the coefficient of variation approaches one, i.e., $CV \to 1$, indicating that the channel gain $\|\mathbf{h}_{mk}\|^2$ becomes a deterministic constant (Fig. 3)[22]. In particular, since $\|\mathbf{h}_{mk}\|^2$ is the sum of N independent and i.i.d. random variables $|h_{mk,n}|^2$, each with finite means and variances, according to the low of large numbers, the sum converges to its expected value as N increases[52].

Thus, the fluctuations due to the small-scale fading diminish because the randomness of individual channel gains averages out over a large number of antennas[22]. This averaging effect causes the channel gain to stabilize around its mean, i.e., channel hardening.

Like co-located mMIMO and CFMM, channel hardening enhances communication and sensing performance in CF-ISAC systems. It leads to more predictable and stable wireless channels as distributed AP antennas increase, reducing the impact of small-scale fading[22]. This results in deterministic channel gains, simplifying channel estimation and reducing the need for frequent CSI updates[22]. This is particularly beneficial in CF-ISAC systems, where accurate and real-time CSI is essential for reliable data transmission and precise sensing tasks such as localization and target detection. The deterministic channels improve the effectiveness of linear processing techniques like maximum ratio transmission (MRT) and maximum ratio combining (MRC), enabling efficient beamforming for communication and sensing without complex algorithms[22][5]. Additionally, channel hardening also allows more efficient power control and resource allocation based on large-scale fading, optimizing the trade-off between sensing accuracy and communication throughput[22][5]. Overall, channel hardening in CF-ISAC systems leads to simplified system design, improved SE, and enhanced performance for joint sensing and communication tasks (Section V-A1)[53].

2. **Favorable Propagation:** This refers to the phenomena of the different user-AP channels becoming virtually orthogonal as the number of AP antennas increases[22][50][27][51]. This orthogonality reduces inter-user interference, enhancing system capacity and performance in multi-user communication. Mathematically, the inner product of the two-channel vectors between the m-th AP and the k-th and l-th users (i.e., $\mathbf{h}_{mk}$ and $\mathbf{h}_{ml}$) is $\mathbf{h}_{mk}^H \mathbf{h}_{ml} = \sum_{j=1}^{N} h_{mk,j}^* h_{ml,j}$, which is a sum of N i.i.d. random variables with zero mean and variance $\beta_{mk}\beta_{ml}$[22]. As $N \to \infty$, according to the law of large numbers, $\mathbf{h}_{mk}^H \mathbf{h}_{ml}$ converges to 0, implying that the two-channel vectors become orthogonal (Fig. 3), i.e.,

$$\frac{\mathbf{h}_{mk}^H \mathbf{h}_{ml}}{\sqrt{\mathbb{E}\left\{\|\mathbf{h}_{mk}\|^2\right\}\mathbb{E}\left\{\|\mathbf{h}_{ml}\|^2\right\}}} \to 0 \quad \text{as} \quad N \to \infty. \tag{2}$$

Favorable propagation aligns with small-scale fading models like Rayleigh and Rician, especially when fading is uncorrelated across AP antennas and users[22][50][27][51]. However, it weakens in highly correlated fading, severe shadowing, or densely deployed APs, leading to high spatial correlations. With a large number of AP antennas (50 to 100), it can make user-AP channels nearly orthogonal, reducing inter-user interference by up to \qty100[22][50][27][51].

By minimizing interference, favorable propagation enables APs to serve more users, improving capacity in CFMM[22]. While it does not directly lower AP transmit power, it enhances EE by reducing the power needed to combat interference[22][50][27][51]. It also facilitates effective user grouping with nearly orthogonal channels. Overall, it enhances resource allocation, user fairness, SE, EE, and user selection/grouping while minimizing interference[22][50][27][51].

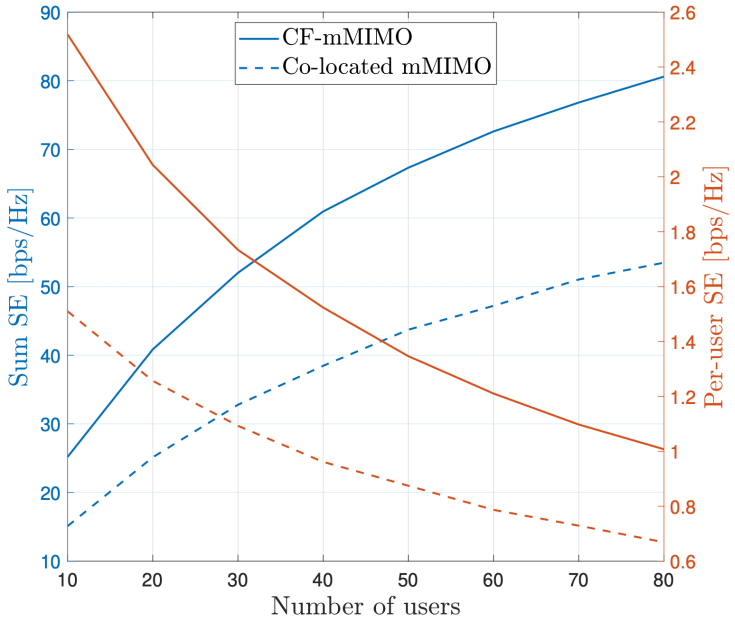

Figure 4. Sum SE (left y-axis) and per-user SE (right y-axis) comparison between CFMM and co-located mMIMO systems with 100 antennas in a coverage area of 1 km^2. In the CF system, the 100 single-antenna APs are uniformly distributed whereas in the co-located system, 100 antenna BS is placed in the cell center. The DL SEs are achieved by assuming conjugate beamforming and statistical CSI knowledge at the users.

4. Performance and Benefits of CFMM over conventional cellular

These include the following:

- *Enhanced coverage:* Multiple distributed APs across a wide area provide users with consistent coverage, even in challenging environments like rural areas or dense urban centers. For example, CFMM systems can reduce outage probability by up to 90% compared to traditional cellular networks, particularly in poor line-of-sight (LoS) conditions[54][55].
- *Improved SE:* CFMM enhances user data rates via spatial multiplexing, achieving 3-to-5 times higher SE than traditional MIMO and exceeding 100 bps/Hz under ideal conditions[26]. As shown in Fig. 4, it outperforms co-located MIMO in both per-user and sum SE, even in dense user scenarios.
- *Reduced interference:* AP cooperation in CFMM minimizes inter-cell interference by eliminating cell boundaries, reducing interference by over 50% compared to conventional cellular systems, particularly for cell-edge users[56].
- *Improved EE:* A large number of APs improves the likelihood of each user being close to an AP. This achieves substantial energy savings by reducing path-loss and enabling lower transmit power levels. For example, energy savings of 30% to 50% are achieved compared to co-located mMIMO[54][56].

The fundamentals of CFMM are well known, thus interested readers refer to[22] and the references therein for further information.

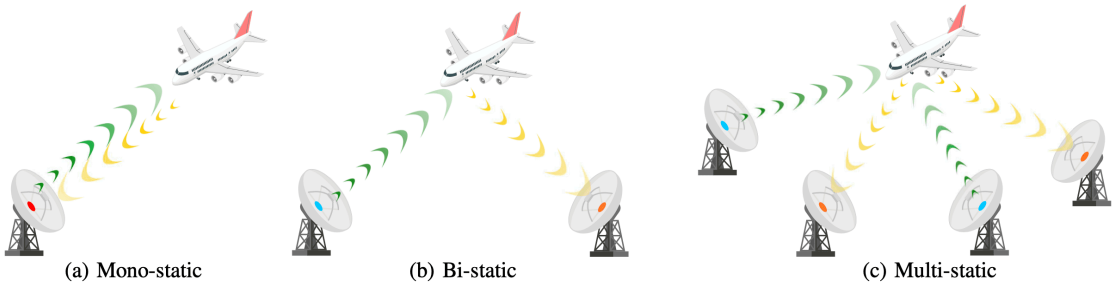

Figure 5. Types of radar/sensing.

B. Fundamentals of Radar Sensing

Radar (short for radio detection and ranging) uses EM waves to detect and estimate object properties. It transmits EM signals toward targets and analyzes their echoes[57][21]. A radar transmitter emits a narrow beam scanning the expected target area, including aircraft, ships, spacecraft, vehicles, astronomical bodies, birds, insects, and rain. When the beam strikes a target, some energy scatters or reflects back to the radar receiver, which can be co-located with the transmitter (mono-static) or at a separate site (bi-static/multi-static) (Fig. 5). Some systems time-share a single antenna for transmission and reception[57][21].

Reflections from targets form the signal of interest, while those from other sources, like the ground or rain, act as interference, degrading detection performance[57][21]. The radar receiver processes echo signals to estimate a target's presence, location, velocity, range, direction, size, and shape. By tracking its position over time, the target's trajectory and path can be predicted. Radar is widely used in defense, automotive, and weather forecasting due to its ability to operate in diverse conditions and measure critical parameters like distance, velocity, and angle.

1. Radar Cross-Section

The RCS quantifies a target's reflecting and scattering characteristics, i.e., a measure of how detectable a target is by radar. It measures the intensity of the incident EM signal reflected back toward the radar by the target[57]. In particular, RCS is the effective area of a target that reflects radar signals back to the source/reader[57]. Mathematically, RCS (σ) is defined as the ratio of scattered power to incident power at a given distance, i.e.,

$$\sigma = \lim_{r \to \infty} 4\pi r^2 \frac{P_{\text{scatter}}}{P_{\text{incident}}}, \tag{3}$$

where r is the distance between the radar and the target, $P_{scatter}$ is the power scattered by the target back toward the radar, and $P_{incident}$ the power incident on the target[57]. RCS depends on the target's size, shape, material, radar frequency, incidence angle, and polarization. Larger, metallic objects typically have higher RCS, while smaller ones have lower values (e.g., an insect: 10^{-5} m^2, a large ship: 10^6 m^2). Higher RCS aids detection at greater distances, whereas low RCS targets require more sensitive radar systems[57]. Table I lists approximate RCS values for common objects[58][59][60].

doi.org/10.32388/8SSIYA

Object	Approximated RCS (m^2)
Insect	$10^{-6} - 10^{-5}$
Bird (e.g., pigeon)	0.01
Human (standing, broadside)	1
Car (sedan, broadside)	$10 - 100$
Large truck	$100 - 200$
Commercial aircraft (e.g., Boeing 747)	$30 - 1000$
Cargo aircraft	Up to 100
Small combat aircraft	$2 - 3$
Large combat aircraft	$5 - 6$
Large ship (e.g., cargo ship, tanker)	$10^5 - 10^6$

Table I. Approximated RCS values of common objects.

2. Clutter

Clutter refers to unwanted radar echoes/interference from objects that are not the intended targets, such as the ground, buildings, trees, or weather phenomena like rain and snow[57]. These reflections can disrupt radar systems by masking or obscuring the identification of intended targets, particularly small or low-RCS objects. Although the effect of clutter on detection can be comparable to that of noise, clutter is influenced by the environment, frequency, and transmitted signals, which may result in a distinct profile from noise[57]. To model the clutter, the Weibull, log-Weibull, log-normal, and K-distributions are commonly employed[61]. To reduce the impact of clutter, the radar systems use clutter rejection techniques[57]. These include moving target indication, Doppler filtering, constant False alarm rate, clutter maps, polarization diversity, and synthetic aperture radar[57].

3. Signal Transmission

Radar systems emit EM signals in the radio or microwave frequency bands[57][21][62][63]. These signals are transmitted through antennas, which convert electrical energy into EM waves. The frequency of the transmitted signal can vary depending on the application, but typical radar systems use frequencies ranging from several megahertz (MHz) to gigahertz (GHz). The frequency of the signal determines both the range and resolution of the radar system. Two common types of radar exist based on the transmitted signals, i.e., continuous wave radar and pulsed radar[62][63].

- *Continuous wave radar:* A continuous signal is transmitted, and the reflected signal is continuously measured. This is often used for measuring velocity (Doppler radar).
- *Pulsed radar:* This transmits short bursts of radio waves, then listens for the return signal. This allows the system to measure the time delay between transmission and reception, which can be used to calculate distance.

4. Types of Sensing

Radar sensing/systems can be classified into three groups based on the spatial relationship between the transmitter and receiver, i.e., mono-static, bi-static, and multi-static sensing/configurations (Fig. 5)[57][21][64]. Each configuration presents unique advantages,

limitations, and challenges in radar signal processing, hardware design, and system performance.

- *Mono-static radar:* This is characterized by a co-located transmitter and receiver pair, often sharing the same antenna (array) for transmission and reception (Fig. 5a). It thus requires full-duplex (FD) operation[57]. However, the simultaneous transmission and reception can introduce strong self-interference (SI), necessitating SI cancellation techniques[65][66]. Alternatively, the receiver should be isolated from the transmitter to protect it from the high SI. However, some modern systems use sophisticated duplexers to allow simultaneous transmission and reception at different frequencies or polarization states[57]. This configuration is widely used in most radar applications due to its simplicity in design and ease of signal processing[57]. Due to the co-located or shared antennas, this has less hardware complexity compared to other configurations. Mono-static radars benefit from well-developed signal processing algorithms, including pulse compression, Doppler processing, and clutter suppression[57]. The transmitter and receiver co-location allows for precise range measurements, with accuracy dependent on the pulse width or bandwidth[57]. Monostatic radar often fails to detect objects having a low RCS, which does not reflect much radar energy to the source[57].
- *Bi-static radar:* The transmitter and receiver are separated, i.e., placed at different locations (Fig. 5b)[57]. The separation can vary from short distances to several kilometers, making it suitable for various operational scenarios such as long-range surveillance and covert detection[57]. Accurate synchronization between the transmitter and receiver is critical as the receiver does not have direct access to the transmitted signal, increasing the complexity of the system[57]. External timing sources/techniques (e.g., direct signal reception, Global Positioning System (GPS) timing, or sophisticated signal tracking algorithms) are required to maintain accurate synchronization[57]. As the receiver is separated from the transmitter, it is harder for adversaries to detect and locate the radar system, making bi-static radar more suitable for military surveillance and stealth applications. The transmitter-receiver separation can reduce clutter caused by direct-path reflections (e.g., from the ground or other environmental features)[57]. On the other hand, the RCS of targets can change dramatically with different bistatic angles, making them sensitive to target orientation and geometry[57].
- *Multi-static radar:* This arrangement involves multiple transmitters and receivers distributed over different locations (Fig. 5c)[57]. It leverages spatial diversity and offers significant advantages in terms of target identification, tracking precision, and resistance to jamming or interference[57]. With multiple receivers, multi-static radar systems can triangulate target positions more accurately than mono-static or bi-static radars. This is particularly useful in cluttered or complex environments[57]. Multi-static radar can be configured to produce high-resolution images of targets using techniques such as synthetic aperture radar and inverse synthetic aperture radar, incorporating multiple observations[57]. Jamming becomes substantially more difficult as an adversary has to disrupt many radar links simultaneously. The spatial diversity of receivers also helps to reduce interference from environmental clutter and multi-path reflections[57]. Nevertheless, this configuration necessitates the coordination of multiple radar nodes, increasing the complexity of the hardware, signal processing, and communications infrastructure. Additionally, precise synchronization between multiple transmitters and receivers is challenging, particularly in dynamic or mobile environments[57].

5. Target Parameter Estimation Techniques

Radar sensing detects targets and estimates parameters such as range, velocity, and angle of arrival (AoA)[57]. Various signal processing techniques enable accurate target parameter estimation:

- *Range estimation:* Matched filtering maximizes the signal-to-noise ratio (SNR) by correlating the received signal with a transmitted signal template. In pulse radar, this identifies target presence and range. The received signal is modeled as

$$y(t) = \alpha s(t - \tau) + n(t), \tag{4}$$

where α is the reflection coefficient, τ is the time delay, $s(t)$ is the transmitted signal, and $n(t)$ is noise. The matched filter's peak at $t = \tau$ determines the target's range[57].

- *Velocity estimation:* Doppler processing determines the radial velocity of moving objects via the Doppler shift Δf_D, which is proportional to velocity. The fast Fourier transform (FFT) converts the received time-domain signal into the frequency domain, where velocity is inferred from spectral peaks[57].
- *AoA estimation:* AoA is determined by analyzing the direction of the reflected signal at the radar receiver. Common methods include:
    1. **Monopulse radar** – this adds extra radio signal encoding to provide accurate directional information. It compares signal intensities from multiple beams or antennas for precise angular location.
    2. **Beamforming** – in phased-array radars – steers beams and processes received signals to determine target direction.
    3. **Subspace-based methods** – techniques like multiple signal classification (MUSIC) and estimation of signal parameters via rotational invariance (ESPRIT) improve AoA accuracy.

III. Integrated Sensing and Communication

ISAC is an emerging paradigm integrating sensing and communication into a unified framework[5]. Unlike traditional systems where these functions operate separately, ISAC leverages its synergy to enhance SE, reduce hardware costs, and enable new applications by sharing resources like spectrum, power, and hardware.

A. Fundamentals of ISAC

ISAC combines sensing and communication within a single system using shared hardware, spectrum, and signal processing techniques[5]. Since radio waves can simultaneously transmit data and extract environmental information from echoes, ISAC exploits this dual capability[5]. However, a key challenge arises: communication systems require highly random signals for maximum channel capacity[67], while radar systems rely on deterministic signals for accurate sensing[57]. This random-deterministic conflict is a fundamental challenge in ISAC, making its research critical for next-generation wireless networks[5].

Integration can be complete or partial, depending on the application. For instance, wireless sensor networks require hardware integration, surveillance radar systems need signaling integration, and cognitive radars rely on spectrum integration[5]. ISAC systems are categorized into four types based on their integration level[5].

- *Level 1 - Spectral coexistence:* This basic integration shares spectral resources between separate communication and sensing systems, minimizing mutual interference while allowing independent operation.
- *Level 2 - Co-located hardware:* In addition to spectrum sharing, this level combines communication and sensing on a shared hardware platform, improving resource efficiency while maintaining distinct operations.
- *Level 3 - Joint signaling and processing:* This level deeply integrates communication and sensing using a common waveform and unified signal processing, enabling seamless operation and performance gains through joint optimization.
- *Level 4 - Perceptive networks:* This is the highest level of integration. A perceptive network is developed by integrating radar-sensing capabilities into wireless communication networks. This level facilitates a fully synergized system capable of catering to emerging connectivity, sensing, and beyond needs in future networks.

Regardless of integration level, ISAC aims to (i) reduce hardware complexity by unifying communication and sensing, minimizing antennas, transceivers, and spectrum use; (ii) enhance SE by coordinating both functions in the same frequency band to minimize interference; and (iii) improve efficiency through joint optimization, reducing energy consumption[5].

B. ISAC Design Philosophy

All ISAC systems combine and jointly design sensing and communication functions to achieve direct trade-offs and mutual benefits[5][4][68]. To illustrate this, consider a general ISAC system with a BS equipped with an M-element uniform linear array (ULA), serving K single-antenna users and tracking targets. The BS transmitted signal at the l-th time slot, denoted as $\mathbf{x}(l) \in \mathbb{C}^{M\times 1}$, can be expressed as

$$\mathbf{x}(l) = \sum_{k=1}^{K} \sqrt{\rho}\mathbf{w}_k q_k(l) + \sqrt{1-\rho}\mathbf{s}(l), \tag{5}$$

where $\mathbf{w}_k \in \mathbb{C}^{M\times 1}$ and $q_k(l)$ denote the communication beamforming vector and the l-th time slot data for the k-th user. The sensing signal, $\mathbf{s}(l) \sim \mathcal{CN}(\mathbf{0}, \mathbf{R}_s)$, follows a complex Gaussian distribution with covariance matrix $\mathbf{R}_s = \mathbb{E}\{\mathbf{s}\mathbf{s}^H\} \succeq \mathbf{0}$. This covariance matrix is designed to extend the DoF of the BS transmit signal, enhancing the system's sensing performance[5]. Finally, $\rho \in [0, 1]$ represents the power allocation or priority factor between communication and sensing, determining the balance and priority between these two functionalities[5].

Based on priority, ISAC designs are classified into three design philosophies: (i) Communication-centric design with high ρ ($\rho \to 1$), (ii) Sensing-centric design with low ρ ($\rho \to 0$), and (iii) Joint design with moderate ρ[68].

1. *Communication-centric design:* This design adapts existing communication systems for dual communication and sensing[69]. Since standard communication signals are not optimized for sensing, advanced processing techniques are utilized to enhance performance. The approach prioritizes communication while extracting target information from signal echoes with minimal modifications.
2. *Sensing-centric design:* Sensing takes priority over communication, with radar as the primary function and communication as a secondary task[70]. For example, communication symbols can be embedded in radar waveforms, ensuring accurate sensing while meeting communication needs. However, the embedded symbols within the sensing signal must not compromise the accuracy or reliability of the primary sensing function, ensuring dependable detection and measurement while simultaneously meeting communication requirements[70].
3. *Joint design:* Here, the signal is designed to assign equal or well-balanced priorities to both sensing and communication, enabling improved trade-offs between the two functionalities. This approach allows for a more flexible resource allocation framework between sensing and communication tasks. As a result, the joint signal design provides greater flexibility and higher DoF, effectively balancing the requirements of both sensing and communication[71].

These ISAC design concepts push conventional communication-only wireless networks to a new dimension[5]. Sensing capabilities, in particular, may become a standard component in future wireless networks, which can be auxiliary or essential for many users and applications. Conversely, sensing data can enhance communication performance. For example, sensing-aided vehicle beamforming and resource management can improve signal quality and optimize network resources, leading to more efficient and reliable communication in dynamic environments[5]. Additionally, sensing-enabled mobile networks can continuously sense their environment and provide traffic monitoring, weather forecasting, and human activity recognition services. This sensing data develops intelligence for the ISAC network and its associated applications, such as smart homes, transportation, and cities[5].

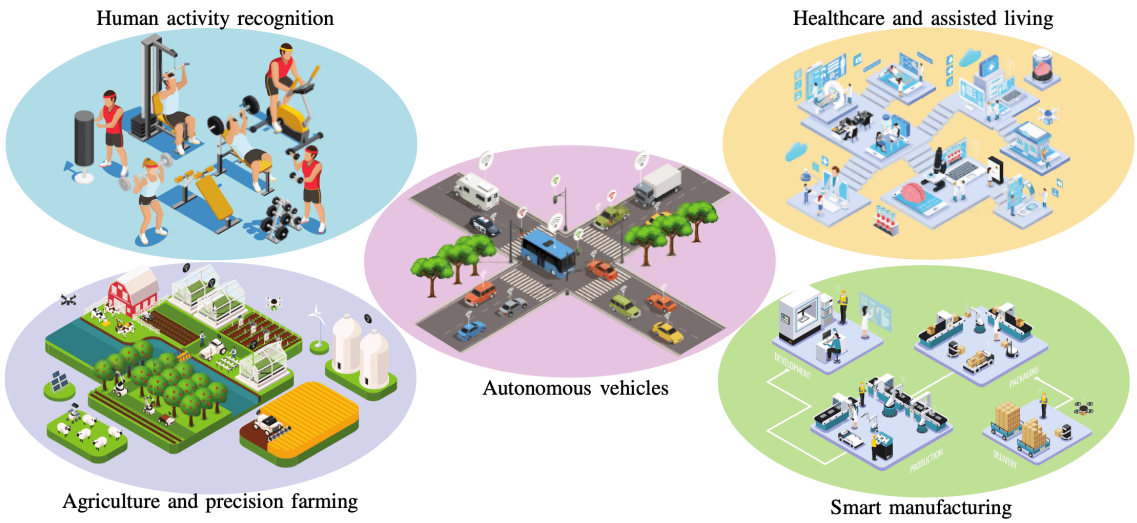

Figure 6. ISAC applications.

C. Sensing Metrics in ISAC

In ISAC, sensing metrics, such as sensing rate/SE, Cramér-Rao bound (CRB), and transmit/receiver beampattern gain, are critical in evaluating the performance of the sensing functionality[72][73][74][57][75][76][77][78][79]. These metrics assess the system's ability to precisely detect and estimate parameters of interest while reflecting the inherent trade-offs between sensing and communication operations[72][73][74].

1. Sensing SE

The sensing SE, measured in bps/Hz, reflects the amount of information the ISAC system acquires about its environment/targets, such as target range, velocity, or angle[72][73][74]. The sensing rate is defined as the mutual information (MI) between the transmitted signal and received reflections/echoes[72][73][74]. For example, consider an ISAC BS with M transmit and M receiver antennas. The received echo signal at the receiver over L symbols can be given as

$$\mathbf{Y} = \mathbf{G}\mathbf{X} + \mathbf{Z} \in \mathbb{C}^{M\times L}, \tag{6}$$

where $\mathbf{X} \in \mathbb{C}^{M\times L}$ is the transmitted signal, $\mathbf{G} \in \mathbb{C}^{M\times M}$ is sensing channel or the target response matrix[57], and $\mathbf{Z}$ is the additive white Gaussian noise (AWGN) matrix at the ISAC BS with independently distributed elements, i.e., $\sim \mathcal{CN}(0, \sigma^2)$. Thus, the sensing MI at the receiver can be given as[74]

$$I(\mathbf{Y}; \mathbf{G}|\mathbf{X}) = M \log_2\left(\det\left(\frac{1}{\sigma^2}\mathbf{X}^H\mathbf{R}_G\mathbf{X} + \mathbf{I}_L\right)\right), \tag{7}$$

where $I(X;Y|Z)$ is the MI between X and Y conditioned on Z, $\mathbf{I}_L$ is an identity matrix of size $L \times L$, and $\mathbf{R}_G = \mathbb{E}\{\mathbf{G}\mathbf{G}\}/M$. Thus, the achievable sensing SE in bps/Hz is defined as[80][81][78][82]

$$\mathcal{S}^{\text{Sen}} = \max_{\text{Tr}(\mathbf{X}\mathbf{X}^H)\le p_{\max}} \frac{M}{L}\log_2\left(\det\left(\frac{1}{\sigma^2}\mathbf{X}^H\mathbf{R}_G\mathbf{X} + \mathbf{I}_L\right)\right), \tag{8}$$

where $p_{\max}$ is the maximum allowable transmit power at the ISAC BS. Alternatively, the sensing SE can be approximated as $\mathcal{S}^{\text{Sen}} \approx \log_2(1 + \text{SINR}^{\text{Sen}})$, where SINR^{Sen} is the sensing signal-to-interference-plus-noise ratio (SINR)[80][81][78][82].

A higher sensing rate indicates greater information extraction per unit time, which is critical for accurate and rapid estimation of target parameters[80][81][78][82]. On the other hand, the optimal sensing waveform based on maximizing the sensing rate has the same estimation performance as the optimal sensing waveform based on minimizing the mean-square error (MSE)[80]. It offers a broader perspective than accuracy metrics like CRB[80]. Consequently, a high sensing rate is essential for many real-time applications, including autonomous vehicles, surveillance radar systems, healthcare monitoring, and environmental monitoring. In these applications, the volume of sensed information is often more crucial for decision-making than individual measurement precision. For example, autonomous vehicles require frequent updates to avoid collisions and navigate dynamic environments. A high sensing rate in surveillance radar systems allows for quick identification and tracking of fast-moving objects. In healthcare monitoring, sensing efficiency is crucial for accurate and continuous measurements of vital signs.

In addition, the quality of target parameter estimation is also proportional to the sensing SE or corresponding sensing SINR[80][81][78]. Improved sensing SE enhances target parameter estimation through proper echo signal processing[80][81][78][83]. Moreover, sensing SE enables parameter estimation using both transmit and receive beampatterns, helping to reduce interference between targets. However, achieving a high sensing rate necessitates careful allocation of system resources such as power and bandwidth, which are frequently shared with communication in ISAC systems[80][81][78][82].

2. CRB

The CRB is the lower bound for the variance of an unbiased estimator designed to estimate a certain parameter and serves as a theoretical limit on the precision of parameter estimation in statistical signal processing[75]. Hence, it offers insights into the maximum achievable accuracy for estimating parameters such as target range, velocity, and angle in ISAC systems[57][75]. Minimizing the CRB thus results in improved target parameter estimation[57][75].

The CRB is derived from the Fisher information matrix (FIM), which quantifies the sensitivity of the likelihood function to changes in the estimated parameters. Mathematically, the CRB for estimating the parameter $\hat{\theta} = [\theta_1, \ldots, \theta_N]^T$ is given by[75]

$$\mathrm{CRB}(\theta_n) = [\mathbf{F}^{-1}(\hat{\theta})]_{nn}, \tag{9}$$

where $\mathbf{F}(\theta)$ is the FIM. In particular, the CRB is a lower bound for the minimum variance unbiased estimation, i.e., $\mathrm{Var}(\hat{\theta}_n) \geq \mathrm{CRB}(\theta_n)$, where $\mathrm{Var}(\hat{\theta}_n)$ is the estimation variance and $\hat{\theta}_n$ is the estimated value of θ_n [57][75]. The elements of the FIM are computed as the expected value of the second derivatives of the log-likelihood function $p(\mathbf{Y};\theta)$ with respect to θ and is given as $[\mathbf{F}(\theta)]_{n,m} = -\mathbb{E}\left\{\frac{\partial^2 \ln(p(\mathbf{Y};\theta))}{\partial\theta_n \partial\theta_m}\right\}$, where $\mathbf{Y}$ is the received echo signal (6). From (6), $\mathbf{Y} \sim \mathcal{CN}(\mathbf{GX}, \sigma^2\mathbf{I}_M)$, and hence the $\{n,m\}$-th element of $\mathbf{F}(\theta)$ can be expressed as [84][85]

$$[\mathbf{F}(\theta)]_{n,m} = \frac{2M}{\sigma^2}\mathrm{Re}\left\{\mathrm{Tr}\left(\frac{\partial(\mathbf{GX})}{\partial\theta_n}\frac{\partial(\mathbf{GX})^H}{\partial\theta_m}\right)\right\}. \tag{10}$$

This indicates how strongly the parameters θ influence the observations $\mathbf{Y}$ [57][75]. A higher Fisher information corresponds to more precise parameter estimation and a lower CRB [57][75].

In sum, the CRB is a key metric for evaluating sensor performance, designing signal processing schemes, and optimizing ISAC systems [86][87][88]. It sets theoretical benchmarks for estimation algorithms, resource allocation, and waveform design. For instance, minimizing the CRB for sensing parameters while preserving communication quality helps balance communication-sensing trade-offs [86][87][88].

3. Beampattern Gain

Sensing beampattern gains are a key ISAC metric, determining how energy is directed (transmit) and signals are analyzed (receive) [76][77][78][79]. The transmit beampattern shapes energy radiation for efficient target illumination, while the receive beampattern, optimized via

sensing combiners, enhances echo reception [76][77][78][79]. These patterns are crucial for optimizing sensing, target detection, and communication efficiency in ISAC systems [76][77][78][79][81][89][90]. Thus, the three pivotal beampattern gains are

$$p_t(\theta) = |\mathbf{a}^H(\theta)\mathbf{x}|^2, \tag{11a}$$
$$p_r(\theta) = |\mathbf{u}^H\mathbf{b}(\theta)|^2, \tag{11b}$$
$$p_c(\theta) = |\mathbf{u}^H\mathbf{b}(\theta)\mathbf{a}^H(\theta)\mathbf{x}|^2, \tag{11c}$$

where $\mathbf{x} \in \mathbb{C}^{M\times 1}$ is the transmitted signal, $\mathbf{a}(\theta) \in \mathbb{C}^{M\times 1}$ and $\mathbf{b}(\theta) \in \mathbb{C}^{M\times 1}$ are the transmit and receiver steering vectors that capture the array responses from direction θ, and $\mathbf{u} \in \mathbb{C}^{M\times 1}$ is the combiner at the receiver. First, (11a) is the transmit beampattern gain and illustrates how the transmitted energy disperses as a function of angle θ. Second, (11b) is the receiver beampattern gain and encapsulates the sensitivity of the ISAC system across different angles during the reception of reflected energy. Finally, (11c) is the combined beampattern gain and offers a combined representation, integrating the effects of transmission and subsequent reflection processing.

Note that in CF-ISAC, the beampattern gains, eq. (11), must be computed at multiple APs. These distributed gains from the APs provide a significant advantage over traditional co-located ISAC[76][91]. Unlike co-located ISAC, which relies on a single viewpoint (e.g., a BS) and primarily estimates target angles, CF-ISAC leverages spatial diversity to refine both angular and distance localization (Fig. 14). By coherently combining beampattern gains â€“ whether from transmission, reception, or both â€“ CF-ISAC mitigates directional ambiguities and improves localization accuracy[91]. In a multi-static scenario, optimizing transmit beampatterns at transmitting APs and enhancing received beampatterns at sensing APs provide reliable data for CPU-level processing. This spatial diversity enhances sensing accuracy, robustness, and detection reliability in dynamic and multi-target environments[91].

Since each AP must evaluate local beampattern gains and exchange information with the CPU for precise target localization, this advantage comes at the cost of increased computational complexity and coordination overhead[76][91]. However, computing beampattern gains at all APs may be unnecessary as a well-placed subset can achieve near-optimal localization while reducing system overhead[76][91]. The required number of APs depends on factors such as target count, visibility, desired localization precision, and AP distribution. Generally, three or more APs with sufficient angular separation are needed for 2D localization, while additional APs enhance robustness in multi-target scenarios and mitigate uncertainties from noise and obstructions.

D. ISAC Applications

ISAC has a wide range of applications, including automotive, healthcare, smart cities, and industrial automation (Fig. 6)[5][2].

1. ISAC for Autonomous Vehicles

Self-driving vehicles need both high-resolution radar sensing for obstacle detection and reliable communication for V2X connectivity. This fusion can transform the transportation industry by enhancing navigation safety, highway capacity, and traffic flow while reducing fuel consumption, pollution, and accident rates[92][93]. In particular, autonomous vehicles acquire ambient information while exchanging data with roadside units (RSUs), other vehicles, and pedestrians[92][93]. Conversely, ISAC-aided V2X can offer environmental information for quick vehicle platooning, secure and seamless access, and simultaneous localization and mapping, addressing EM compatibility and spectrum congestion challenges[92][93].

2. Human Activity Recognition

Computing systems can monitor, evaluate, and assist people daily by recording their behaviors, making activity recognition essential[94]. Wireless signal fluctuations, influenced by static and moving objects and human actions, can detect activities such as presence, proximity, falls, sleep, breathing, and more. These capabilities have significant applications in healthcare and transportation[94]. For instance, detecting a driver's blink rate with high-resolution sensors can help identify drowsy driving, enhancing road safety. Additionally,

integrating sensing capabilities into commercial wireless devices like Wi-Fi can identify occupant behaviors, creating innovative, human-centric environments[94].

3. Smart Manufacturing (Industry 4.0)

Communication and sensing enable the automation of production lines in smart manufacturing[95]. Modern factories feature interconnected machinery, robotic arms, and autonomous systems collaborating in real-time to ensure efficiency and precision. Machines communicate wirelessly and sense their environment, detecting factors like vibrations, temperature changes, and product quality. This dual functionality supports predictive maintenance, allowing machines to identify potential failures proactively, reducing downtime, and minimizing repair costs[95].

4. Healthcare and Assisted Living

Integrated solutions for continuous monitoring and real-time communication are vital for improving patient outcomes and elderly care[96]. These systems enable remote monitoring by collecting health data such as heart rate, blood pressure, and oxygen levels and transferring it to healthcare providers for real-time evaluation. This allows personalized care and timely interventions without requiring hospital visits[96]. In assisted living, sensors track daily activities, detect falls, and identify abnormal behavior, such as prolonged inactivity, alerting caregivers or medical professionals during emergencies. Hospitals can also benefit by optimizing patient flow, medical equipment usage, and staff coordination, enhancing healthcare delivery[96].

5. Agriculture and Precision Farming

Critical environmental conditions, such as soil moisture, nutrient levels, weather, and crop health, play a key role in agriculture[97]. For instance, soil sensors can monitor moisture content in real-time, enabling irrigation systems to adjust water usage automatically. Drones equipped with ISAC technology can survey large fields, detect plant diseases, pest infestations, and growth patterns, and use this data to apply pesticides or fertilizers precisely. This integration of communication and sensing reduces resource waste, such as water and chemicals, while boosting crop yields and sustainability[97].

E. Evolution of the ISAC Networks

Conventional ISAC systems, or *link-/system-level ISAC designs*[1], focus on single- or dual-BS cellular architectures[5][1][98][99][71][83][100][101][81][102][82]. However, they face challenges such as inter-cell interference, limited coverage due to obstructions and high-frequency attenuation, and the mismatch between sensing and communication ranges caused by two-hop path-loss[103][104].

To address these issues, *network-level ISAC* leverages multiple ISAC transceivers across cells to enhance both communication and sensing[105][106]. This approach enables high-throughput, ultra-reliable communication and precise, high-resolution sensing.

For sensing, network-level ISAC extends coverage beyond single-cell systems using multi-static sensing, where each BS processes both local radar echoes and target-reflected signals from other BSs or users. For communication, transceiver collaboration enables techniques like CoMP transmission, reducing inter-cell interference and ensuring robust multi-user connectivity. By integrating sensing and communication at task, data, and signal levels, network-level ISAC improves resource management, signal strength, interference mitigation, and coverage quality[107].

While network-level ISAC systems effectively mitigate inter-cell interference and improve communication and sensing system performance, they face several challenges[105][106]. These challenges include

- *Coverage issues at cell edges:* Users located at the edges of cells, who may not fully benefit from coordinated transmissions, experience lower performance due to imperfect alignment of signals from multiple BSs.
- *Scalability limitations:* As CoMP involves coordination across multiple BSs, scaling the system becomes increasingly complex and resource-intensive, especially as the number of users and BSs grows.
- *High fronthaul overhead:* CoMP requires significant fronthaul resources to coordinate multiple BSs, as they need to exchange CSI and user data in real-time. This creates a high dependency on fronthaul links, which can be a bottleneck in practical deployments.
- *Vulnerability to imperfect CSI:* The effectiveness of CoMP heavily depends on accurate and up-to-date CSI shared between BSs. However, acquiring and sharing precise CSI is challenging, especially in dynamic environments where delays, estimation errors, and quantization can degrade performance.
- *High computational complexity:* The coordination between multiple BSs in CoMP systems requires complex algorithms for joint beamforming, power allocation, and user scheduling. As the number of coordinated BSs and users increases, the computational demands grow significantly.
- *EE:* CoMP can be energy-intensive due to the need for high-power transmission and centralized coordination across BSs.

IV. Cell-Free Integrated Sensing and Communication

CFMM offers a robust platform for implementing many sensing systems, including mono-static and multi-static sensing (Section II-B4). Unlike mono-static, multi-static sensing in CF-ISAC systems eliminates the requirement for FD nodes while also providing diversity gain via distributed/non-colocated transmitters and receivers, i.e., it can achieve improved sensing performance using multiple uncorrelated sensing observations[6][7][8][9][10][11][12][13][14]. To implement multi-static CF-ISAC, the concept of network-assisted CFMM[108] can be leveraged to identify the ISAC transmitters and receivers. Furthermore, CF-ISAC can use orthogonal waveforms to exploit the intrinsic spatial diversity of target RCS, enhancing sensing accuracy in estimating target parameters and detection probability[20][109].

A. Key Features of Cell-Free ISAC

The key features of CF architecture, such as DASs, seamless handovers, enhanced interference management, AP cooperation, and scalability, make CF-ISAC an appealing solution for future wireless communication and sensing[6][110][7][111][112][53][113][8][9][14][114]. These characteristics not only allow for joint optimization of communication and sensing but also improve communication coverage and sensing accuracy[6][110][7][111][112][53][113][8][9][14]. In addition, CF-ISAC systems utilize wireless resources more efficiently than traditional co-located ISAC architectures, making them crucial for next-generation applications such as 6G networks, smart cities, self-driving cars, healthcare, and industrial IoT.

1. Distributed Antenna Systems

In CF-ISAC, APs are geographically distributed across the coverage region (i.e., DAS) rather than concentrated at a single BS, offering distinct advantages for both communication and sensing[115][116][20]. This distribution provides significant spatial diversity, improving communication by mitigating spatially correlated fading, shadowing from obstacles, and reducing end-to-end transmission distances[22][18][27]. For sensing, it enhances environmental perception by enabling multi-static sensing (Section IV-B), which improves resolution and accuracy[6][110][7][111][112][53][113][8][9].

Distributed APs also provide wider and more uniform coverage, removing the cell-edge issue encountered in traditional co-located systems[22][18][27]. In CF-ISAC, the users and targets are simultaneously served by multiple APs, enhancing both communication quality and sensing precision. In addition, because APs are distributed across the network, users/targets are always in close proximity to multiple

APs[6][110][7][111][112][53][113][8][9][14]. This effectively lowers latency and provides more reliable connections. This is especially important in time-sensitive ISAC applications such as autonomous driving, where communication and sensing must occur with minimal latency[5].

2. Seamless Handover and User/Target-Centric Operation

In traditional cellular networks, each user is served by a single BS. When a user moves from one cell (or BS) to another, a handover is necessary[22][18][27]. This can result in delays, signal overhead, and even connection interruptions[22][18][27]. However, in CF-ISAC, the concept of no cell boundaries assures that a user/target is not tied to a specific AP. Instead, numerous APs cooperate to serve the user/target concurrently. When the user/target moves, nearby APs take over, eliminating the requirement for a hard handover[22][18][27]. This improves reliability, reduces latency, and boosts overall network performance. Furthermore, unlike cellular networks, the system does not require frequent switching between BSs (APs), making it appropriate for applications with significant mobility, such as vehicular networks or drones[5]. In a CF-ISAC network, seamless handover ensures uninterrupted communication while performing environmental sensing. It eliminates signal degradation or interruption even when users or targets move between various AP regions.

User/target-centric operations optimize network resources based on the specific location and requirements of users (for communication) and targets (for sensing)[22][23]. Unlike traditional cell-centric networks, where each cell serves a user independently, CF-ISAC networks serve each user/target via a nearby set of APs, effectively placing them at the center of a dedicated serving cluster. This cluster, formed based on selected criteria such as serving performance and network efficiency, consists of APs contributing useful signals/data. A two-stage process can further refine clustering, first using large-scale fading statistics to form a base cluster, then optimizing it with scheduling or power allocation algorithms per time slot[22][23]. This approach ensures optimal resource allocation, enhancing communication quality and sensing coverage.

3. Interference Management and Resource Allocation

Managing interference between sensing and communication tasks, as well as between different users and targets, is one of the most significant issues in co-located ISAC[5]. In particular, the concurrent operation of these tasks in the same frequency spectrum often leads to conflicting requirements, as optimizing for communication performance might reduce sensing accuracy, and vice versa[5]. Furthermore, interference among multiple users and sensing targets exacerbates the issue, emphasizing the importance of developing sophisticated beamforming and resource allocation algorithms to balance these competing objectives while minimizing cross-task and inter-user interference.

Nevertheless, in CF-ISAC, the distributed nature and cooperative architecture of APs can substantially reduce interference. By allowing APs to collaborate and share information, the system obtains more spatial diversity and flexibility in resource management, improving interference suppression[22][18][27]. Advanced techniques such as CoMP processing, interference alignment, and beamforming can be used to reduce cross-user/target interference by ensuring that signals from various users or sensing tasks do not overlap[22][18][27]. The distributed design also enables more precise control over beamforming and power allocation, lowering the likelihood of unintentional interference between sensing and communication operations[22][18][27].

4. AP Cooperation and Synchronization

In a CF network, numerous distributed APs collaborate to serve users and execute sensing tasks in a collaborative and coordinated manner[22][18][27]. This collaboration is key to realizing the benefits of CF-ISAC, which uses the same infrastructure for both communication and environmental sensing. The advantages of AP cooperation include increased communication and sensing coverage, reduced interference, and efficient use of network resources.

AP cooperation can be achieved through cooperative beamforming, in which APs coordinate their transmissions to improve signal strength while minimizing interference[22][18][27]. In sensing, this improves spatial resolution and coverage by combining signals from multiple APs to create a more accurate representation of the environment. This is especially critical in situations where targets may be hidden from certain APs or where multipath reflections make sensing more difficult[6][110][7][111][112][53][113][8][9][14]. In communication, coordinated APs improve data throughput and reduce the risk of signal dropouts during transmission. Furthermore, the CPU is crucial in AP cooperation, acquiring data from APs, processing it, and coordinating transmissions to improve both communication and sensing[22][18][27]. The CPU can dynamically assign AP resources (e.g., power, spectrum, and time slots) in response to real-time demands.

B. Cell-Free ISAC Versus Link-Level ISAC Design

The CF-ISAC designs with multi-static sensing provide significant advantages over link-level mono-static or bi-static ISAC designs. These advantages stem primarily from their distributed architecture and the ability of multiple APs to participate in both communication and sensing[6][7][8][9][10][11][12][13][14].

Feature	CF-ISAC sensing (Multi-static)	Conventional ISAC sensing (Mono/bi-static)
Sensing coverage	Broader with fewer blind spots	Limited to single/double viewpoint
Sensing accuracy	High due to triangulation from multiple points	Lower and limited by fewer viewpoints
Robustness	High resilience to node failure	Vulnerable to single-point failure
SNR and sensitivity	Improved through signal diversity	Limited SNR with sensitive to noise
Scalability	Easily scalable across APs	Difficult to scale
Multi-path exploitation	Can utilize multi-path signals for extra information	Often treats multi-path as interference
Multi-target tracking	More effective and can track multiple targets	Limited in tracking multiple targets simultaneously
Interference management	Better due to spatial diversity	More susceptible to interference
Resource optimization	Highly flexible for joint communication-sensing	Limited flexibility
NLoS handling	More effective due to multiple angles	Often requires LoS or favorable geometry

Table II. A compression of sensing in CF-ISAC and conventional ISAC.

1. Improved Sensing Coverage

CF-ISAC with multi-static sensing involves multiple distributed sensing transmitter-receivers (APs) covering a wide area. This provides a larger coverage than link-level ISAC design, which normally relies on a single or two locations for sensing. Furthermore, link-level ISAC design is frequently restricted by LoS conditions. CF-ISAC avoids blind spots and provides reliable coverage across broader regions.

2. Improved Sensing Accuracy

CF-ISAC utilizes measurements from multiple distributed nodes, resulting in improved triangulation and more accurate localization or target detection. Furthermore, cross-correlating observation from multiple sources can also greatly improve resolution, precision, and detection. On the other hand, because link-level ISAC design relies on one or two points of view, their precision is restricted, and they are more likely to overlook fine data details of the target, e.g., position, movement, or characteristics.

3. Enhanced Robustness and Resilience

Multi-static sensing in CF-ISAC improves system robustness by enabling continued operation even in the event of node failures or interference, ensuring the system remains functional under challenging conditions. The distributed structure provides robustness and reliability when mono-static/bi-static systems fail due to obstruction, occlusion, or physical limitations. In link-level ISAC design, mono-static/bi-static sensing is more susceptible to single-point failures, i.e., if the BS fails to perform sensing, the system loses all sensing capabilities.

4. Improved SNR and Detection Sensitivity

CF-ISAC systems employ coherent combining and diversity gain to improve sensing SNR, leveraging multiple observations through received signals. This can assist in detecting weak or distant targets that may have been overlooked in mono-static or bi-static systems. Mono-static/bi-static systems, on the other hand, are limited by the signal SNR or dual channels, i.e., transmitting and receiving, reducing detection sensitivity, particularly in challenging environments (e.g., dense urban areas and cluttered environments).

5. Distributed and Scalable System Architecture

Multiple APs in CF-ISAC perform joint communication and sensing in a distributed and scalable manner, i.e., each AP contributes to both tasks, optimizing network resources and providing seamless scalability. In co-located ISAC, communication and sensing tasks are centralized and less flexible, i.e., they lack inherent scalability compared to CF networks when expanding coverage or adding new sensing nodes.

6. Multi-Path (Macro-Diversity) Exploitation

CF-ISAC can leverage multi-path propagation or macro-diversity, which involves signals reflected from multiple points and surfaces, providing more information about the environment and targets. This is especially beneficial in indoor or cluttered environments with plenty of reflections. However, link-level ISAC design may fail to effectively utilize multi-path signals, often treating them as interference rather than meaningful information.

7. Simultaneous Multi-Target Tracking

By leveraging the user-centric (UC) nature of the CFMM architecture, CF-ISAC allows different APs to focus on distinct targets and combine the gathered data, enabling simultaneous monitoring of multiple targets. This approach enhances the efficiency and accuracy of multi-target tracking, particularly in dynamic environments with moving objects. In contrast, the link-level ISAC design with a single BS has limited capacity to manage multiple targets simultaneously, leading to performance degradation due to signal overlap or occlusion.

8. Interference Management

CF-ISAC can use the spatial diversity of distributed architecture to reduce interference. In particular, observations/measurements from several angles and distances aid in differentiating targets from noise. Because of the limited number of observations in the link-level ISAC design, interference from other communication channels or ambient clutter is more difficult to eliminate.

9. Joint Communication-Sensing Optimization

In CF-ISAC systems, the network may optimize resources (e.g., power, bandwidth) among scattered APs to balance communication and sensing demands. The distributed design provides greater flexibility in distributing resources depending on dynamic demands. For example, sensing in a specific region while maintaining communication quality elsewhere. Nonetheless, co-located ISAC systems have

fewer DoF for joint resource allocation, making it more difficult to accomplish effective communication-sensing trade-offs, particularly in dynamic environments.

10. Non-LoS Capability

In CF-ISAC, multi-static sensing can successfully manage non-LoS (NLoS) conditions as APs provide alternate viewpoints of the target, potentially circumventing obstructions or blockages. In contrast, mono-static/bi-static sensing in the link-level ISAC design relies on LoS or favorable positioning. Thus, obstacles or structures that conceal the target are significant limitations.

In conclusion, multi-static sensing in CF-ISAC systems offers significant advantages in sensing coverage, accuracy, robustness, and flexibility compared to the link-level mono-static or bi-static ISAC design. These benefits make CF-ISAC particularly well-suited for complex, dense, or large-scale future-generation wireless networks. A summary of these aspects is provided in Table II.

V. State of the Art in Cell-Free ISAC

A. Performance Analysis in Cell-Free ISAC

Analytical performance evaluation provides insights into a wireless system's behavior, potential, and limitations under various conditions. It may predict performance without requiring extensive simulations or real-world testing. In CF-ISAC systems, it is crucial for optimizing communication and sensing interactions, guiding resource allocation, balancing trade-offs, ensuring scalability, and assessing real-world feasibility.

Nevertheless, CF-ISAC performance analyses are lacking, except for[117][118][119]. In particular, reference[117] presents a communication and sensing protocol for a CF-ISAC system with a single target, where an AP is allocated to participate in the UL alongside users, delivering a radar signal to the network. This approach models the radar system as a distributed bi-static radar to recover radar echoes from multi-user interference. The cost imposed on the communication system is the loss of an AP, as it is treated as a virtual user in the communication system. Two radar sensing modes are proposed, i.e., sensing during either the UL training period or the data payload segment of the communication frame. A subspace signal model and a corresponding generalized likelihood ratio test (GLRT) are developed to assess detection performance, with expressions for the probability of detection and false alarm presented.

Reference[118] studies a centralized CF-ISAC mMIMO system for single-target detection, where transmit APs serve DL users while steering a beam toward the target in a multi-static sensing setup. A maximum a-posteriori ratio test detector is developed to detect the target amid clutter, with sensing SE as a key performance metric. The study also explores two ISAC signal models—leveraging communication beams for sensing and adding dedicated sensing beams—and proposes a power allocation algorithm to maximize sensing SINR while ensuring minimum communication requirements.

In[119], the performance of multi-user single-target CF-ISAC with transmit APs using MRT precoding is analyzed. Each AP uses locally estimated CSI to design and transmit a superimposed ISAC waveform for user communication, while designated sensing APs process reflected echoes for sensing. A max-min algorithm optimizes transmit power to maximize the weakest user rate while maintaining a predefined signal-to-clutter-plus-noise-ratio (SCNR) threshold at each sensing AP. Achievable user rates and the two-dimensional MUSIC spectrum for target localization are derived, considering CSI errors, spatially correlated Rician fading, and clutter interference. Numerical results demonstrate CF-ISAC's potential with efficient MRT precoders.

1. Case Study and Discussion

This case study evaluates a generalized CF-ISAC system with multiple targets and users, extending beyond existing single-target scenarios (Fig. 7). It examines the interplay between communication and sensing, highlighting key trade-offs.

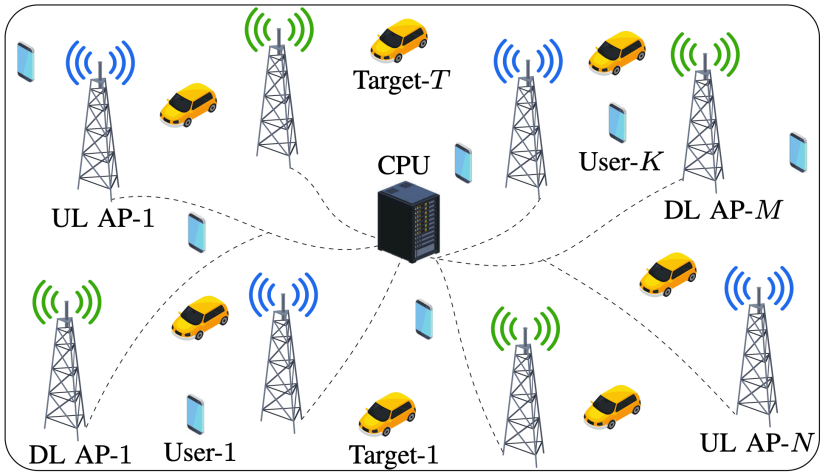

Figure 7. A CF-ISAC system setup with UL and DL APs.

It considers the following model. A CF-ISAC mMIMO system with M DL APs and N UL APs, each with L antennas, serves K single-antenna DL users and detects T targets (Fig. 7). All APs connect to a CPU via fronthaul/backhaul links. DL APs serve users while steering sensing beams toward targets using the same time-frequency resources. UL APs capture reflected echoes for sensing. Analytical expressions for communication SE at users and sensing SE at UL APs for each target are derived, with channel and transmission models and performance evaluation detailed in Appendix A.

Simulation Example: this employs the 3GPP Urban micro (UMi) model for large-scale fading $\zeta_{\mathbf{a}}$, where $\mathbf{a} \in \{\mathbf{h}_{mk}, \mathbf{g}^{\mathrm{d}}_{mt}, \mathbf{g}^{\mathrm{u}}_{mt}\}$, with an operating frequency of $f_c = 3$ Table B.1.2.1[120]. The AWGN variance is modeled as $\sigma^2 = 10\log_{10}(N_0 B N_f)$ dBm, where $N_0 = -174\mathrm{m}/$, $B = 10$ is the bandwidth, and $N_f = 10$ is the noise figure. Additionally, the UL and DL APs are uniformly distributed, while the users and targets are randomly distributed over a 200×200 area.

doi.org/10.32388/8SSIYA

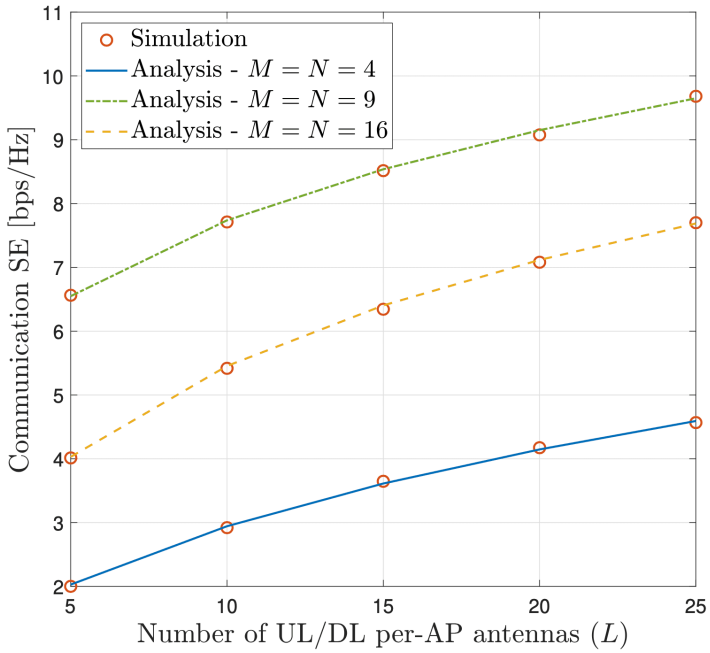

Figure 8. Communication SE versus the number of AP antennas.

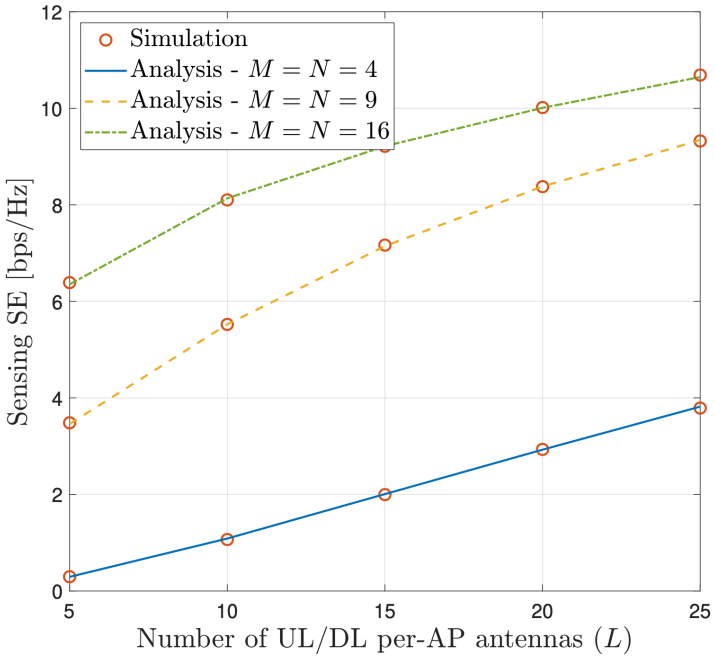

Figure 9. Sensing SE versus the number of AP antennas.

Fig. 8 and Fig. 9 plot the communication SE and sensing SE as functions of the number of UL/DL AP antennas (L), respectively, for different numbers of UL/DL APs, $M = N = \{4, 9, 16\}$. The accuracy of the analytical SEs is validated using Monte-Carlo simulation. In particular, the analytical communication and sensing SE curves and respective Monte-Carlo simulation curves coincide regardless of the simulation

doi.org/10.32388/8SSIYA

setup, validating the accuracy of the derived analytical rate expressions. As observed from both Fig. 8 and Fig. 9, increasing the number of antennas at UL and DL APs results in high communication and sensing SE. This is due to the improved spatial diversity, beamforming gains, and reduced interference. For example, 31.3% and 51.7% communication and sensing SE gains, respectively, can be achieved by increasing the number of antennas from 10 to 20 with $M = N = 9$. Moreover, deploying a higher number of APs provides additional spatial diversity and coverage, further boosting both communication and sensing performance. These insights highlight that denser antenna deployments and increased AP counts are critical for achieving higher spectral efficiency in CF-ISAC systems, leveraging the benefits of distributed antenna arrays and efficient resource allocation.

B. Resource Allocation in Cell-Free ISAC

Resource allocation optimizes bandwidth, power, time, and antennas to meet data demands, support multiple users, ensure fairness, and enhance performance. However, varying requirements across wireless applications make allocation complex. Different networks (e.g., Wi-Fi, LTE, sensor, and energy harvesting) require tailored solutions rather than a one-size-fits-all approach. While standard algorithms address some challenges, others demand customized strategies.

Conversely, CF-ISAC resource allocation faces additional challenges in balancing sensing and communication while managing resources across distributed APs. Their complex distributed nature and joint functionality requirements demand tailored solutions. To address these challenges, various resource allocation schemes have been developed[6][110][7][111][112][53][113][8][9][14][121][12][13][10][11][91]. In particular, many of these studies focus on designing AP beamforming approaches to facilitate efficient resource allocation[6][7][111][9][10][12][53][113][91]. Although traditionally considered a signal processing technique, beamforming in CF-ISAC inherently involves resource management as the AP transmit power is embedded within the beamforming vectors. This integration directly affects how system power is distributed across APs to optimize communication and sensing performance. Thus, beamforming plays a critical role in CF-ISAC resource allocation frameworks.

Reference[6] presents a beamforming design for a multi-user, single-target CF-ISAC system under CSI errors. The beamforming problem is formulated as a sensing beampattern matching MSE minimization, subject to power budget constraints at the APs and user rate requirements. With lower bound user rates over the imperfect CSI, a successive convex approximation (SCA)-based algorithm is proposed. For a single-target CF-ISAC system, references[7][111] propose a max-min fairness joint beamforming design. The approach utilizes two benchmarks: communication-prioritized sensing beamforming and sensing-prioritized communication beamforming, to balance performance between communication and sensing tasks. In[8], a coordinated power control scheme is investigated for CF-ISAC transmitters. The objective is to minimize the total transmit power of the APs while meeting the minimum communication SINR for users and the maximum Cramér-Rao lower bound (CRLB) for target location estimation. Two efficient algorithms based on semidefinite relaxation (SDR) and CRLB approximation are proposed.

Reference[9] examines a multi-user, multi-target CF-ISAC system and proposes vector orthogonal frequency division multiplexing (OFDM) signals to enhance SE, detection resolution, and latency/Doppler estimation accuracy. To estimate the AoAs for multiple targets, a low-complexity grid-searching approach is introduced. Additionally, AP beamforming and power allocation are designed using an alternative Lagrange multiplier algorithm. In[10], a hybrid beamforming architecture for a multi-user, multi-target cooperative CF dual-function radar-communication network is investigated. The hybrid beamforming at APs is designed to maximize the weighted communication sum rate while ensuring the MSE constraint of the beampattern gain for radar sensing. This is achieved through a semi-distributed approach using an alternating optimization (AO) algorithm. In[11], a CFMM system with integrated virtual UL radar is proposed. The radar system operates in the UL, with a subset of APs dedicated to radar transmission alongside user communications. Power control is employed at the APs to manage the interference from the communication system on the radar, incorporating linear interference

constraints into the sum SE and sum-log-SNR policies. Additionally, a low-complexity solution based on the largest large-scale fading heuristic is presented.

In[12], a transmit beamforming design for a single-target, multi-user CF-ISAC system is presented, where a user acts as an adversary attempting to infer the target's position. To overcome this, an expectation-maximization algorithm is offered for estimating the transmitted signal, which is subsequently utilized to create replicas of the transmit beampattern for each AP. A power allocation algorithm is offered to maximize the sensing SNR while meeting the minimum SINR requirements for users in[13]. Thereby, a maximum a posteriori ratio test detector is derived to detect the target using signals received at distributed APs. The studies[14][121] examine DL ultra-reliable low-latency communication (URLLC) in a CF-ISAC system. It proposes an SCA-based power allocation algorithm to maximize the EE of the network while meeting the sensing SINR and communication decoding error probability requirements.

Refernce[110] considers a multi-user, single-target CF-ISAC mmWave mMIMO system with capacity-limited fronthaul links. A power allocation scheme with a fronthaul compression design is proposed that uses hybrid analog and digital precoders, with digital precoders created at the CPU and analog precoders designed at each transmitting AP. Two block coordinate descend (BCD)-based algorithms are presented. In[112], the AP operating mode selection approach is presented for a multi-user, single-target CF-ISAC system. In particular, some APs are dedicated to DL communication, while the remaining APs are utilized for sensing. With closed-form SE and mainlobe-to-average-sidelobe ratio, a max-min fairness problem is formulated to maximize the minimum user SE. For a multi-user, multi-target CF-ISAC system, reference[53] provides transmit beamforming designs to accommodate ISAC, communication-only, and sensing-only scenarios. Three different solutions are presented via the Lagrangian dual transform, the quadratic fractional transform technique, the BCD method, and the SCA method.

In[113], the joint AP mode selection, transmit beamforming, and receive filter designs are investigated for cooperative CF-ISAC networks, where the APs cooperatively serve multiple communication users and detect targets. Three heuristic AP mode selection techniques and an efficient joint beamforming design method are presented. In[91], a new efficient and low-complexity beamforming design for CF-ISAC networks is proposed. The proposed algorithm leverages the augmented Lagrangian model-based Riemannian manifold optimization technique to maximize the communication sum rate while satisfying sensing beampattern gains of multiple targets and per-AP transmit power constraints.

1. Case Study and Discussion

Herein, a beamforming design for a generalized CF-ISAC system (Fig. 10) is provided and evaluated with numerical examples.

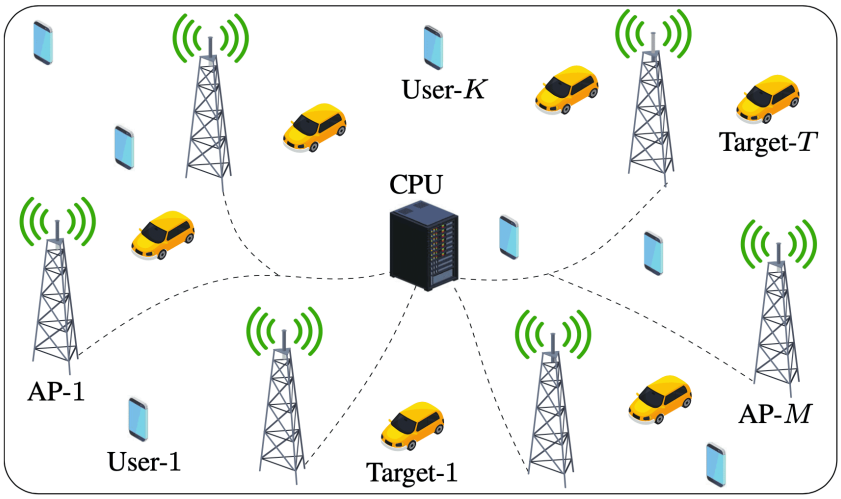

Figure 10. A CF-ISAC system setup.

Fig. 10 investigates a CF-ISAC system compromising M APs, each equipped with L ULA antennas, K single-antenna users, and T potential targets. The CPU connects all APs and coordinates the joint communication and sensing, ensuring time synchronization across all APs[18]. The communication SE at the users and the transmit beampattern gains at the AP towards the targets are utilized to evaluate the communication and sensing performance, respectively. The objective is to maximize the communication SE for the users while satisfying sensing beampattern gain requirements for each target and per-AP transmit power constraints. Interested readers are referred to[91] for comprehensive details on the system, channel, and transmission models, along with the analytical performance evaluation and the associated algorithm.

Simulation Example: The simulation setup is the same as in Section V-A1, excluding the UL APs. The maximum allowable per-AP transmit power is set to $p_{\max} = 30\text{dBm}$, and the required sensing beampattern gain for each target is set to $\Gamma_t^{\text{th}} = 10\text{dBm}$.

doi.org/10.32388/8SSIYA

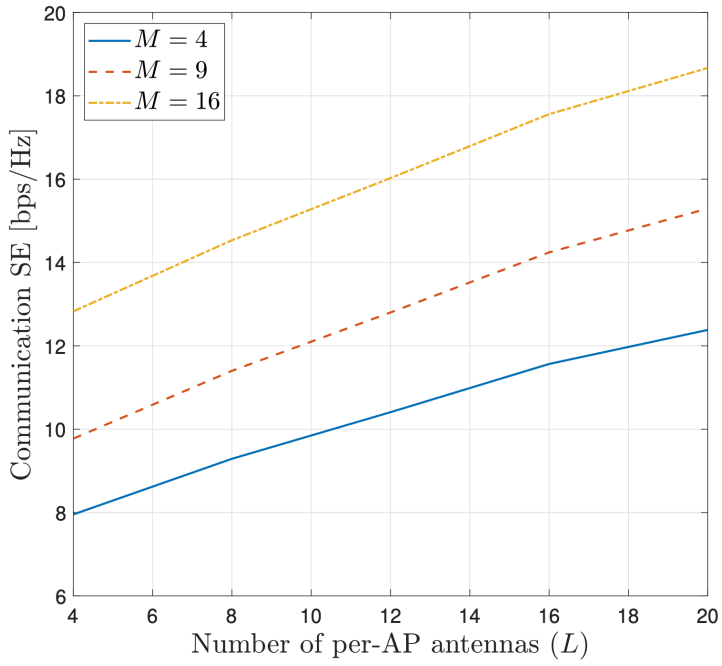

Figure 11. Communication SE versus the number of per-AP antennas for $K = 2$ and $T = 3$.

Fig. 11 plots the communication SE as a function of the number of AP antennas (L) for different numbers of APs, $M = \{4, 9, 16\}$, with $K = 2$ and $T = 3$. Fig. 11 illustrates that, for all values of M, the communication SE increases as the number of AP antennas increases. Additionally, for a given L, a higher value of M results in a higher communication SE. For example, with $M = 16$ and $L = 12$, it provides 53.9% and 25.2% higher communication SE than $M = 4$ and $M = 9$ cases, respectively.

This performance improvement highlights the scalability and flexibility of CF-ISAC systems. Increasing the number of APs enhances spatial diversity, enabling more efficient interference management and resource allocation across multiple users. Furthermore, adding more antennas at each AP improves the beamforming gain, allowing for more precise spatial multiplexing and better signal quality. The distributed nature of CF-ISAC ensures that users benefit from the cooperation of multiple APs, mitigating path-loss and shadowing effects.

doi.org/10.32388/8SSIYA

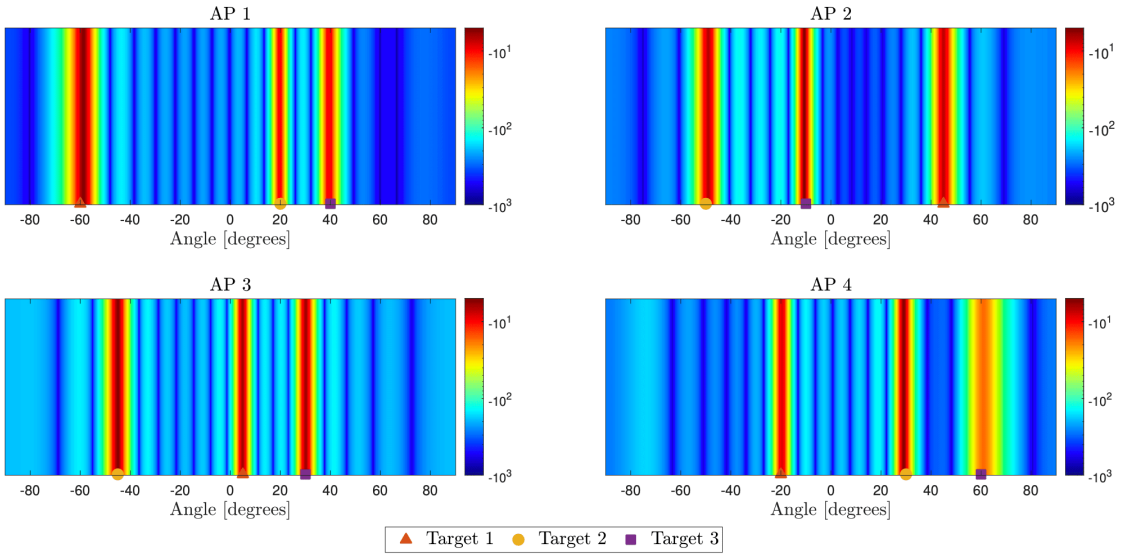

Figure 12. Beampattern gain profiles over a $\pm 90^{\circ}$ angular spread at different APs, illustrating the gain variations and directivity in a color-coded scale for $L = 8$, $M = 4$, $K = 2$, and $T = 3$.

Fig. 12 presents the effects of beamforming gains utilizing $L = 8$ AP antennas with $M = 4$ APs for $K = 2$ and $T = 3$. In particular, Fig. 12 plots directional gain profiles in a color-coded scale to evaluate the performance of beamforming gains at each APs. The direction angles for sensing targets from AP 1, AP 2, AP 3, and AP 4, are set to $\{-60, 20, 40\}^{\circ}$, $\{25, -70, -10\}^{\circ}$, $\{25, -45, 75\}^{\circ}$, and $\{-20, 30, 60\}^{\circ}$, respectively, ensuring coverage of a broad angular range.

The color gradient represents beamforming gain magnitude, with red indicating strong gains from focused energy and blue showing minimal radiated power. Intersecting beampattern gain directions across APs enables precise target localization, a key advantage of CF-ISAC's multi-static sensing over mono-static or bi-static approaches in co-located ISAC (Fig. 14). The distributed APs provide multiple viewpoints, enhancing spatial resolution and mitigating multi-path fading. Overlapping beampattern gains allow for accurate triangulation using AoA information from different perspectives, improving localization accuracy and resilience against blockages and interference. Additionally, if one AP experiences poor signal quality, others compensate, ensuring consistent sensing performance across the coverage area.

doi.org/10.32388/8SSIYA

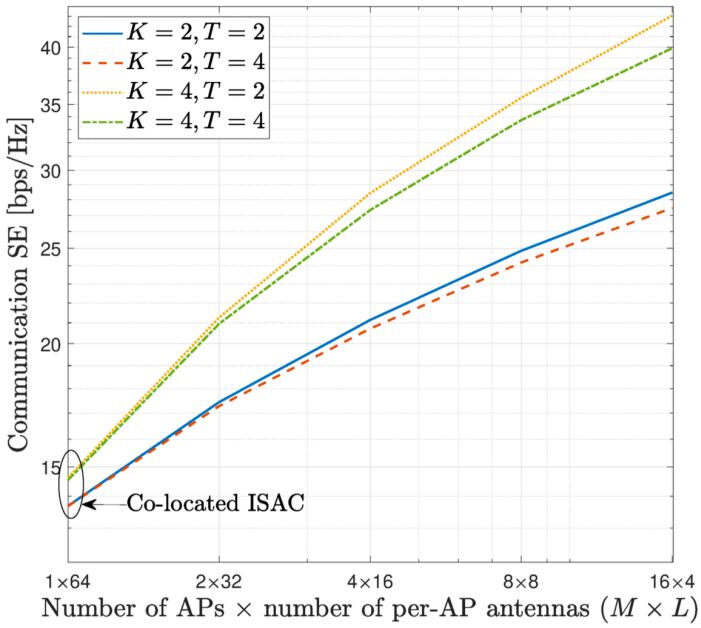

Figure 13. Communication SE comparison between CF-ISAC and co-located ISAC systems for $M \times L = 64$.

Fig. 13 compares the communication SE between CF-ISAC and co-located ISAC systems. In particular, the product of the number of APs and per-AP antennas, i.e., $M \times L$, is kept at 64. The co-located ISAC system corresponds to the $M = 1$ and $L = 64$ setup, while CF-ISAC configurations have $M > 1$. The figure reveals that CF-ISAC systems consistently outperform their co-located counterparts, attributed to micro-diversity gains achieved by spatially distributed APs, leading to reduced path loss and shadowing effects. This distributed nature allows CF-ISAC to provide more uniform coverage and better signal quality than co-located ISAC systems.

Additionally, Fig. 13 also highlights the trade-off between communication and sensing performance. The communication SE decreases when the number of targets increases for the same number of users. This is because more system resources are allocated to sensing tasks with a high number of targets, such as transmit power for target detection and tracking, thereby reducing resources available for communication. This underscores the importance of balancing communication and sensing tasks in ISAC systems to optimize overall performance. With its distributed APs, the CF-ISAC architecture offers flexibility in dynamically managing this trade-off by exploiting spatial diversity and adaptive resource allocation[91].

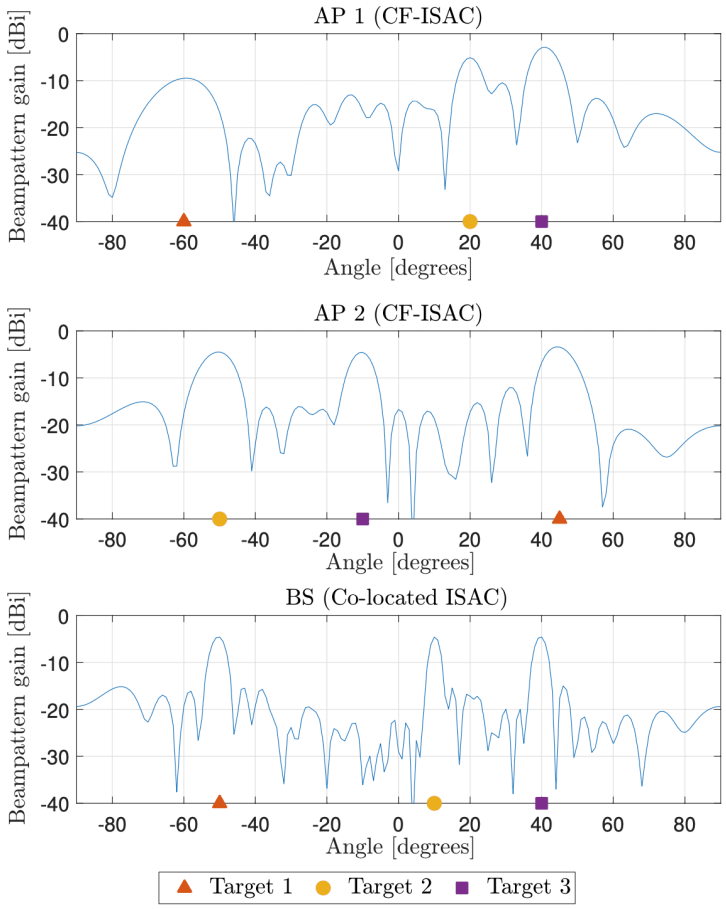

Figure 14. A comparison of directional beampattern gain profiles over a $\pm 90^\circ$ angular spread between CF-ISAC and co-located ISAC systems.

Fig. 14 compares beampattern gains between CF-ISAC and co-located ISAC systems for $T = 3$. The former uses two 16-antenna APs (AP1 and AP2) to perform communication and sensing. In contrast, a 32-antenna, single BS at the center of the coverage area serves the latter. The direction angles for sensing targets from AP1 and AP2 are set to $\{-60, 20, 40\}^\circ$ and $\{45, -50, -10\}^\circ$. In contrast, the co-located ISAC system targets at directions $\{-50, 10, 40\}^\circ$ from the BS.

As shown in Fig. 14, both CF and co-located configurations direct their main lobes toward targets, indicating their locations. However, CF-ISAC offers a key advantage over co-located ISAC by leveraging distributed APs. By combining beampattern gains from multiple APs, CF-ISAC enables precise target localization in both angular and distance dimensions. In contrast, co-located ISAC, with a single viewpoint (i.e., BS), can only determine angular directions. The spatial diversity of CF-ISAC resolves directional ambiguities and enhances position estimation.

Additionally, CF-ISAC supports more flexible and adaptive beamforming as APs cooperate. This enhances localization accuracy and robustness against blockages and interference. In contrast, the single BS may struggle with precise distance estimation in a co-located ISAC system. The distributed architecture is particularly beneficial for dynamic environments requiring precise and resilient target tracking.

doi.org/10.32388/8SSIYA

C. Security Challenges of Cell-Free ISAC

CF-ISAC and ISAC networks face more significant security risks than traditional wireless systems. This is because using information beams to enhance sensing can lead to information leakage, mainly when targets include adversarial entities like eavesdropping UAVs[122]. They not only intercept transmitted data but may also exploit sensing information to disrupt system performance. Conventional countermeasures such as beamforming, sensing covariance matrix design, and artificial noise (AN) transmission can enhance secrecy[123]. However, these solutions must be adapted for CF networks. While deploying more APs and receivers improves spatial diversity, it also increases vulnerabilities to active eavesdropping and pilot signal manipulation, potentially disrupting legitimate sensing.

These CF-ISAC security issues have been studied recently[88][124][125]. In[88], a secure CF-ISAC system with multiple users and a single target, assumed to be an eavesdropper, is considered. The system aims to ensure reliable communication for the users while simultaneously detecting the target using monostatic sensing and degrading the eavesdropper's channel quality. To achieve this, an ISAC waveform embedded with AN is designed to minimize the CRB when estimating the target's direction relative to the APs. Using the SDR method, the CPU optimizes the precoding vectors and AN covariance matrices for each AP. This optimization is constrained to maintain the required SINR for the users while limiting the eavesdropper's maximum SNR. The study reveals an inverse proportionality between the optimal CRB and the user-eavesdropper distance, highlighting the impact of spatial positioning on ISAC performance. In[124], a multi-static sensing model is examined in which multiple eavesdroppers try intercepting confidential information intended for communication users. The authors propose a joint communication and sensing beamforming design aimed at maximizing the sensing SNR while ensuring that the secrecy rate for all communication users remains above a specified threshold. In[125], the security of both communication and sensing is examined in the presence of information and sensing eavesdroppers, who seek to intercept confidential communications and extract target information, respectively. The study formulates a transmit beamforming optimization problem aimed at maximizing the detection probability while adhering to several constraints: SINR constraints for communication users, SNR constraints for information eavesdroppers, detection probability constraints for sensing eavesdroppers, and transmit power limitations for each transmitter. The global optimal solution was obtained using an SDR-based approach.

1. Case Study and Discussion

Here, the resource allocation framework of the CF-ISAC system, Fig. 10, is extended to explore its security aspects. In particular, one or more targets not only serve as objects of interest for the ISAC system but also act as eavesdroppers, attempting to intercept confidential information intended for communication users. It is assumed that a malicious target attempts to decode the information of any user from the received signal. If successful, it can then use the successive interference cancellation (SIC) technique to decode the information of all other users. Therefore, the leakage SEs at the targets for decoding user data are considered for evaluating the security performance. Our goal is to maximize the communication SE for users while meeting the sensing beampattern gain requirements and minimizing the leakage SE to targets/eavesdroppers for any user. This approach ensures that eavesdroppers are unable to decode any user information, thereby securing communication data against eavesdropping.

Simulation Example: The simulation setup is the same as the case study in Section V-B. Moreover, the maximum allowable leakage SE at all targets/eavesdroppers, $\delta_{\max}$, is set to 0.5 bps/Hz.

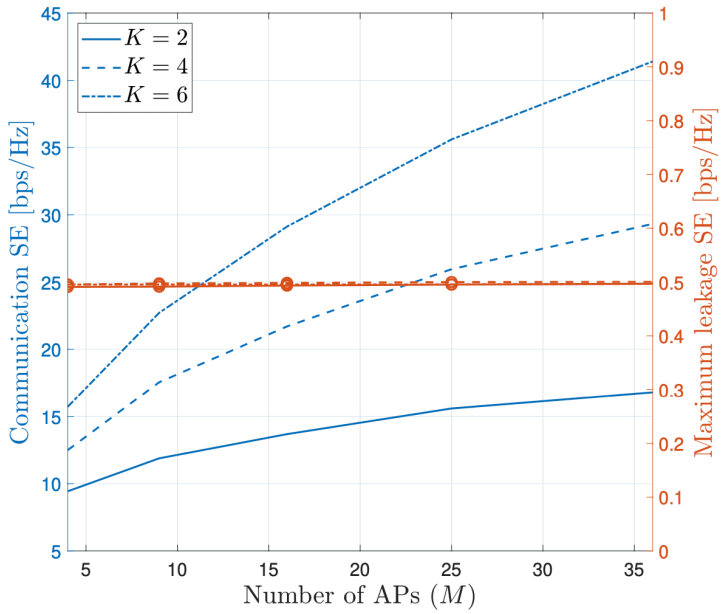

Figure 15. Communication SE and maximum leakage SE as functions of the number of APs.

Fig. 15 shows the impact of the number of APs (M) on both the communication SE (i.e., left y-axis) and the maximum leakage SE at the targets or eavesdroppers (i.e., right y-axis) for different numbers of users, $K = \{2, 4, 6\}$. As the number of APs increases, the communication SE improves significantly due to enhanced spatial diversity, beamforming gains, reduced path loss and shadowing effects, and efficient interference management. The system effectively scales with additional users, utilizing spatial multiplexing and distributed resources to boost spectral efficiency. For instance, at $M = 16$, the system setup with $K = 6$ delivers communication SE gains of 112.8% and 34.2%, over $K = 2$ and $K = 4$, respectively. This demonstrates the CF-ISAC system's capability to accommodate more users while maintaining strong performance.

The secrecy performance, measured by maximum leakage SE at potential eavesdroppers, remains stable across AP densities, indicating effective information leakage prevention. Secure beamforming ensures data protection even as the network densifies. While increasing APs enhances communication SE, maintaining security requires optimized beamforming to suppress leakage SE. These findings highlight CF-ISAC's suitability for secure, scalable wireless networks, including mission-critical IoT, defense, and surveillance applications.

doi.org/10.32388/8SSIYA

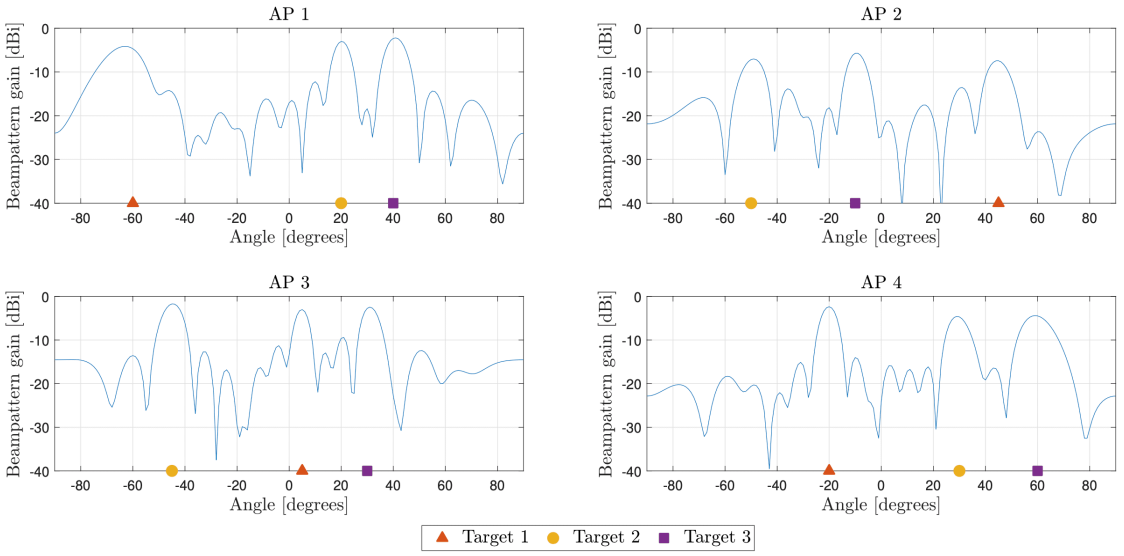

Figure 16. Directional beampattern gain profiles over a Â $\pm 90^{\circ}$ angular spread at different APs.

Fig. 16 plots the directional beampattern gain profiles of the secure ISAC system with $L = 8$, $M = 4$, $K = 2$, and $T = 3$. The subfigures are for beampattern gains at different APs, i.e., AP 1, AP 2, AP 3, and AP-2. The directions of the targets at these APs are set similarly to those in Fig. 12. Fig. 16 shows how the secure beamforming effectively concentrates radiated power in target directions at each AP. This is accomplished by optimizing communication and sensing beamforming at each AP, minimizing interference among users and targets, and reducing information leakage at the eavesdroppers.

The sharpness of the main lobe peaks indicates precise beam steering, ensuring high sensing accuracy and reliable communication. Meanwhile, the depth of the troughs and sidelobe attenuation reflects the system's ability to suppress undesired signal leakage, reducing the probability of interception by eavesdroppers. The varying beampatterns across APs highlight the distributed and cooperative nature of CF-ISAC, where each AP dynamically adjusts its beamforming to optimize both performance and security. These results confirm the system's robustness in jointly managing sensing and secure communications, making it suitable for applications requiring both high detection accuracy and strong data confidentiality.

D. User/Target-Centric Cell-Free ISAC

Scalability is a key obstacle in deploying CF networks, as the computational complexity and fronthaul capacity demanded by each AP to process and share data signals for all users grow linearly (or even faster), with the number of users. As an alternative, UC-CF has been introduced[41]. In this approach, each user is served by a subset of APs (an AP cluster) offering the most favorable channel conditions, leading to the formation of overlapping cooperation clusters across the network. As a result, each AP must dynamically collaborate with different APs when serving different users, all within the same time and frequency resources. In CF-ISAC networks, AP clustering can be performed from the user point of view[126], or from the target point of view[127]. In the former scheme, user scheduling is carried out across different APs, with each communication user being served by a cluster of APs, while all APs collaborate on the sensing task. The latter introduces a target-centric approach, where the surveillance area is divided into non-overlapping regions. Then each area is sensed by a subset of APs. The target-centric approach presents an intriguing research direction for supporting multi-target sensing in a distributed manner. However, forming AP clusters that account for network dynamics, along with managing collaboration between overlapping APs in the sensing function, remains a challenging task that requires further investigation.

doi.org/10.32388/8SSIYA

VI. Key Challenges and Open Research Directions

This section discusses key challenges, open research directions, and future trends of CF-ISAC technology.

A. Key Challenges in Cell-Free ISAC

1. Multi-Target Sensing

Accurately detecting and tracking multiple targets simultaneously remains a significant challenge in CF-ISAC systems. This complexity arises from the need to differentiate overlapping echoes from separate targets across distributed APs, often leading to ambiguities in detection and tracking. While the distributed nature of APs provides additional spatial diversity, it also complicates coordination[127]. A potential solution is to divide the scan area into disjoint regions, with each region monitored by designated APs. To enhance robustness, APs can participate in multiple regions, increasing both redundancy and detection reliability.

A critical aspect of this approach is the design of an effective coordination protocol. This protocol must ensure that adjacent radar cells, i.e., disjoint regions, are not scanned simultaneously, thereby minimizing mutual interference and reducing the risk of target misdetection in overlapping areas. Ideally, radar cells scanned concurrently should be spatially separated to mitigate cross-region interference. Techniques such as time-division multiplexing and spatial scheduling can be employed. Additionally, advanced signal processing algorithms, including compressed sensing and sparse recovery, can resolve targets in dense environments, further enhancing multi-target detection capabilities[127].

2. Synchronization

Synchronization is crucial for CF architecture to ensure all APs operate in a coordinated manner[22][18][27]. It guarantees coherent transmission and reception among APs. It encompasses timing, frequency, and phase alignment, which are critical for achieving high data rates in communication and precise target detection in sensing applications[22][18][27]. Lack of proper synchronization leads to signal misalignment, resulting in interference, degraded communication quality, and reduced sensing accuracy. This misalignment can severely impair joint beamforming operations, causing beam misdirection that diminishes the quality-of-service (QoS) for users and the resolution of radar sensing. In practical deployments, maintaining synchronization is challenging due to hardware imperfections, oscillator drifts, and propagation delays[128].

To address these challenges, CF-ISAC systems may employ disciplined local oscillators synchronized via Global Positioning Systems (GPS) or fronthaul-based coordination protocols[128]. However, as the number of spatial distributed APs increases, achieving and maintaining precise synchronization becomes more complex. Non-ideal clock behaviors, such as phase noise and jitter, introduce additional errors that distort processed echo signals, degrading detection accuracy and overall system performance[128].

3. Interference Management

This is a critical challenge in CF-ISAC systems due to the simultaneous operation of communication and sensing functions within the same spectral resources[129]. The dual spectrum use can lead to co-channel interference, where communication signals interfere with sensing operations and vice versa. This interference can degrade both data throughput and target detection accuracy.

Effective interference management requires adaptive beamforming, interference alignment, and spectrum sharing protocols[129][130]. Adaptive beamforming can dynamically steer communication and sensing beams to minimize interference, while interference alignment techniques can exploit the spatial dimensions to separate interfering signals. Additionally, resource allocation strategies, including dynamic spectrum access and power control algorithms, are essential to optimize the coexistence of communication and sensing functionalities.

4. Fronthaul Capacity and Latency

The performance of CF-ISAC networks hinges on the fronthaul infrastructure linking distributed APs to the CPU. Bandwidth, latency, and reliability constraints in fronthaul links can hinder real-time coordination, data transmission, and sensing[131]. These challenges are especially critical in CF-ISAC systems, where high-throughput communication and real-time sensing demand ultra-reliable, low-latency connections[131].

In CF-ISAC systems, fronthaul latency directly affects synchronization accuracy, beamforming efficiency, and sensing timeliness. High latency can lead to outdated CSI and delayed sensing feedback, degrading adaptability in dynamic environments[131]. Limited bandwidth further constrains CSI and sensing data exchange, impairing communication and sensing performance.

To mitigate these limitations, CF-ISAC systems can integrate edge computing and distributed processing, reducing reliance on centralized processing and easing fronthaul bottlenecks. Fronthaul compression, latency-aware scheduling, and optimized resource allocation further enhance efficiency. Additionally, advanced fronthaul technologies such as millimeter-wave and optical fiber links can help meet stringent latency and bandwidth demands.

B. Open Research Directions and Future Trends

1. Network-Assisted Cell-Free ISAC

In network-assisted CFMM, the CPU coordinates the operation modes of APs, i.e., UL or DL, virtually realizing FD operation within CF architecture[132]. In particular, this centralized coordination enables the dynamic assignment of APs to either transmit DL signals or receive UL signals/echoes based on real-time network demands, user distribution, and channel conditions. Compared to conventional CFMM, this can enhance SE and mitigate interference across the network[132][133]. Network-assisted CF-ISAC is thus particularly promising for meeting both UL and DL communication demands while simultaneously sharing resources with sensing functionality[132][133]. This approach supports flexible multi-static sensing, where APs can be adaptively assigned to transmit DL sensing signals or receive UL echoes based on network demands. Additionally, this framework facilitates the simultaneous transmission and reception of UL and DL signals[134][135].

However, communication and sensing tasks can interfere significantly. UL communication signals at UL-operating APs contain both echo-sensing signals and cross-link interference from DL APs. Similarly, sensing signals received at UL APs experience interference from both UL and DL communications, degrading sensing performance. Consequently, resource allocation in the network-assisted CFMM system must be optimized to design UL and DL power control coefficients and configure AP mode operations to meet both communication and sensing demands. One potential solution is to divide the UL APs into two disjoint groups, with one dedicated to sensing and the other serving UL communications.

2. New Antenna Technologies and Cell-Free ISAC

To fully exploit spatial resources and further enhance ISAC performance, fluid antennas—also known as movable antennas—have been introduced in the literature[136][137][138]. The core concept of fluid antennas is that their position can be optimized within a specified region, providing spatial diversity with fewer RF chains in a relatively small space[139]. This could be beneficial at the user terminal, given the limited available space. Therefore, deploying fluid antennas at the APs and multi-antenna users in CFMM networks provides new spatial DoF to enhance the performance of ISAC applications. However, several concerns need to be addressed. Firstly, channel estimation and the optimization of position changes are major challenges. Additionally, high-dimensional optimization problems are expected to increase in complexity to synergize with ISAC scenarios. While fluid antenna systems exploit a series of spatially correlated signals, artificial intelligence can be incorporated into the design process due to its powerful ability to identify hidden correlations.

A recent antenna technology that is gaining significant attention is holographic MIMO (HMIMO), which refers to an affordable, transformative wireless planar structure made up of sub-wavelength metallic or dielectric scattering particles. This structure has the ability to manipulate EM waves in a way that aligns with specific goals[140]. The HMIMO surface can function as a transmitter, receiver, or reflector, making it a versatile solution for creating reconfigurable wireless environments. The authors in[141] have developed an artificial intelligence (AI)-based framework that integrates HMIMO APs into CF networks to enable efficient power allocation for beamforming in the desired direction, leveraging ISAC. This framework optimally distributes power for beamforming by selectively activating the necessary grids within the serving HMIMO APs in the network to meet user demands. To achieve this, the authors formulate an optimization problem aimed at maximizing the sensing utility function. This approach enhances the SINR of the received signals, improves the sensing SINR of the reflected echo signals, and boosts EE, ensuring effective power allocation.

3. Cell-free ISAC and Near-Filed

The increasing interest from both academia and industry in the previously underutilized upper mid-band spectrum (7â€“24 GHz)[142][143][4], also known as FR3, has underscored the significance of extremely large mMIMO (XL-MIMO) antenna arrays. When either the physical aperture of the antenna array is large or the wavelength is small, the Fraunhofer distanceâ€”defined as $\frac{2D_{\text{array}}^2}{\lambda}$, where D_{array} is the aperture size and λ is the wavelengthâ€”can become substantial[4]. As a result, near-field propagation conditions may arise when serving UE at shorter distances. While this phenomenon is not observed in 5G, it is a potential implication for 6G.

When a beam is concentrated on a location in the near field, the spherical curvatureâ€™s transverse variations cause the focus to dissipate beyond a certain distance. As a result, the beam pattern in the near field takes on a spotlight-like shape, whereas in the far field, it expands outward conically. A significant advantage of near-field beam focusing is that an XL-MIMO system can distinguish user devices based on both distance and angle. This enhances the richness of multi-user MIMO channels and boosts the overall sum capacity[144][145]. More importantly, by capturing both angular and distance information from the incoming spherical wavefronts in the near-field region of the antenna array, high-resolution three-dimensional location estimation becomes achievable[4]. These near-field characteristics are particularly beneficial in mmWave and sub-THz frequency bands, where the wavelength is short. However, the near-field regionâ€™s boundary, known as the Fraunhofer distance, is typically limited to just a few tens of meters for a conventionally-sized 6G base station in the upper mid-band[145][146]. **The question now is how CFMM, with its low-cost and typically small antenna aperture size at APs, can leverage near-field sensing and localization?**

In[147], the authors highlight that deploying coordinated subarrays with only a few meters of separation enables near-field beam focusing without requiring a large continuous aperture. This approach also benefits sensing and localization. While each subarray captures locally planar wavefronts, combining signals from multiple subarrays reveals spherical curvature, similar to the CFMM framework, where arrays are distributed over large areas. However, effective near-field simulation requires careful AP placement and robust fronthaul and synchronization infrastructure to ensure coherent coordination. These requirements may increase power consumption, potentially offsetting EE gains in future 6G networks, making EE a crucial design consideration.

4. Consolidation of Complementary Technologies into Cell-Free ISAC

To enhance CF-ISAC performance, integrating complementary technologies has gained traction. Notably,[148] proposed a NOMA-aided CF-ISAC architecture to improve connectivity and efficiency. Focusing on a single-radar sensing scenario, the study jointly optimizes user pairing and beamforming to maximize the minimum achievable communication rate while meeting sensing requirements. Future research could extend this work by incorporating statistical CSI-based designs that account for channel estimation or exploring multi-target scenarios with both instantaneous and statistical approaches.

In[149], an FD CFMM system enhanced by a single reconfigurable intelligent surface (RIS) was investigated. The RIS was utilized to assist in maximizing the weighted sum of radar and communication SINRs. To achieve this, a joint optimization framework was proposed, encompassing the design of radar and communication receive beamformers, UL transmission powers, DL sensing beamformers, and RIS reflection coefficients. The systemâ€™s performance can be further enhanced by deploying multiple RIS within the network to expand coverage across a larger area. Additionally, integrating advanced technologies such as beyond-diagonal RIS and stacked metasurfaces presents a compelling avenue for future research and development.

The utilization of multiple UAVs in a CFMM architecture for ISAC systems with dedicated sensing signals has been explored in[150]. Specifically, three deployment scenarios for the UAVs were considered: mobile UAVs, tethered UAVs, and fixed UAVs. for all scenarios, a transmit precoder that jointly optimizes the sensing and communication requirements subjected to power constraints was designed.

5. Machine Learning-Based Techniques for CF-ISAC

Unifying sensing and communication in CFMM systems enhances performance, reduces spectrum congestion, and lowers costs by sharing hardware resources. However, these benefits rely on optimally designed ISAC waveforms, precoders, detectors, and estimators. Achieving optimal designs involves complex multi-objective optimization due to inherent sensing and communication trade-offs. Moreover, the unified designs and real-time implementation of CF-ISAC based on classical model-based analytical techniques may often become sub-optimal due to model inadequacy or incompleteness. On the other hand, the Pareto-optimal algorithms and solutions for the multi-objective optimization problems that apply to CF-ISAC may be entirely unknown in some instances. They may also be prohibitively complicated in computations or practically non-viable in implementations.

ML-based techniques have emerged as powerful and efficient data-driven alternatives to classical model-based signal processing and optimization[151][152][153]. Deep learning, in particular, is well-suited for CF-ISAC, where multiple conflicting objectives must be jointly optimized[154]. For instance, deep learning can be used to design efficient unified beamformers that balance sensing and communication goals[154].

These benefits accrue due to data-driven CF-ISAC techniques extracting features from high-dimensional multimodal data, leveraging its embedded low-dimensional structures for model learning[155]. The multimodal sensory information in CFMM channels can enhance model-driven CF-ISAC designs and optimizations. Retaining 3D data structures improves the accuracy and generalization of learning-based models, even with limited datasets. Deep learning can also aid in jointly estimating communication and sensing channel parameters, including CSI acquisition, data decoding, and target localization through delay, Doppler, and angular-domain parameter estimation.

Deep learning enhances adaptivity and enables intelligent network features in CF-ISAC. Applications include autonomous vehicles, localization, human activity detection, environmental monitoring, object tracking, smart surveillance, and wide-area imaging.

VII. Conclusion

This article explored the emerging CF-ISAC paradigm, which integrates CF and ISAC to enhance SE, EE, and sensing in future wireless networks. It began with a review of CF and ISAC fundamentals and their integration into CF-ISAC, highlighting its unique characteristics. The benefits of multi-static sensing and key features of CF-ISAC systems were then examined. Current developments were categorized into performance analysis, resource allocation, security, and user/target-centric designs, providing a comprehensive literature survey and case studies. Finally, the article outlined key challenges, open research directions, and emerging trends, offering valuable insights for future advancements.

Appendix A. Performance Analysis in Cell-Free ISAC

A. Channel Model

For the system setup in Fig. 7, block flat-fading channel models are considered. During each fading block, $\mathbf{h}_{mk} \in \mathbb{C}^{L\times 1}$, $\mathbf{g}^{\mathrm{d}}_{mt} \in \mathbb{C}^{L\times 1}$, and $\mathbf{g}^{\mathrm{u}}_{nt} \in \mathbb{C}^{L\times 1}$ are the channel vectors from the m-th DL AP to the k-th user, the m-th DL AP to the t-th target, and the t-th target to the n-th UL AP, respectively. Moreover, $\mathbf{F}_{mn} \in \mathbb{C}^{L\times L}$ represents the channel between the m-th DL AP and the n-th UL AP. All channels are assumed to be independent quasi-static Rayleigh fading, which remains constant during the coherence interval. A unified representation of all channels is given as

$$\mathbf{a} = \zeta_{\mathbf{a}}^{1/2}\tilde{\mathbf{a}}, \tag{12}$$

where $\mathbf{a} \in \{\mathbf{h}_{mk}, \mathbf{g}^{\mathrm{d}}_{mt}, \mathbf{g}^{\mathrm{u}}_{mt}\}$, $\zeta_{\mathbf{a}}$ accounts for the large-scale path-loss and shadowing, and $\tilde{\mathbf{a}} \sim \mathcal{CN}(\mathbf{0}, \mathbf{I}_L)$ captures the small-scale Rayleigh fading, which is static during one coherence interval. With time division-duplexing mode for both channel estimation and data transmission, CSI can be estimated by employing orthogonal pilots[22], which is highly accurate. Thus, perfect CSI availability is assumed.

B. Transmission Model

The transmitted signal at the m-th DL AP, $\mathbf{x}_m \in \mathbb{C}^{L\times 1}$, is given as

$$\mathbf{x}_m = \sum_{k=1}^{K} \mathbf{w}_{mk} q_k + \sum_{t=1}^{T} \mathbf{s}_{mt}, \tag{13}$$

where $q_k \in \mathbb{C}$ represents the intended data symbol for the k-th user with unit power, i.e., $\mathbb{E}\{|q_i|^2\} = 1$, and $\mathbf{w}_{mk} \in \mathbb{C}^{L\times 1}$ is the m-th DL AP transmit beamforming vector for the k-th user, and $\mathbf{s}_{mt} \in \mathbb{C}^{L\times 1}$ is the dedicated sensing signal at the m-th DL AP for the t-th target[81]. It is also assumed that q_k and $\mathbf{s}_{mk}$ are independent of each other[81].

The received signal at the k-th user is given as

$$\begin{aligned} y_k &= \sum_{m=1}^{M} \mathbf{h}_{mk}^H \mathbf{x}_m + z_k \\ &= \underbrace{\sum_{m=1}^{M} \mathbf{h}_{mk}^H \mathbf{w}_{mk} q_k}_{\text{Desired signal}} + \underbrace{\sum_{i\neq k}^{K} \sum_{m=1}^{M} \mathbf{h}_{mk}^H \mathbf{w}_{mi} q_i}_{\text{Multi-user interference}} \\ &\quad + \underbrace{\sum_{t=1}^{T} \sum_{m=1}^{M} \mathbf{h}_{mk}^H \mathbf{s}_{mt}}_{\text{Sensing signal interference}} + \underbrace{z_k}_{\text{AWGN}}, \end{aligned} \tag{14}$$

where $z_k \sim \mathcal{CN}(0, \sigma^2)$ is the AWGN at the k-th user.

The UL APs use the reflected signals from the targets, i.e., the target echoes, to extract the target's state information[81]. The received signal at the n-th UL AP, i.e., $\mathbf{y}_n \in \mathbb{C}^{L\times 1}$, is given as

$$\begin{aligned} \mathbf{y}_n = & \underbrace{\sum_{m=1}^{M} \mathbf{F}_{mn} \mathbf{x}_m}_{\text{Direct-link interference}} \\ & + \underbrace{\sum_{t=1}^{T} \mathbf{g}^{\mathrm{u}}_{nt} \alpha_t \sum_{m=1}^{M} (\mathbf{g}^{\mathrm{d}}_{mt})^H \mathbf{x}_m}_{\text{Target echoes}} + \underbrace{\mathbf{z}_n}_{\text{AWGN}}, \end{aligned} \tag{15}$$

where $\mathbf{z}_n \sim \mathcal{CN}(\mathbf{0}, \sigma^2 \mathbf{I}_L)$ is the AWGN at the n-th UL AP and $\alpha_t \in \mathbb{C}$ is the complex amplitude of the t-th target reflection, accounting for the round-trip path-loss and the RCS of the target[156]. Specifically, path-loss accounts for signal attenuation over distance, while the RCS determines how much power is reflected toward the radar receiver, depending on the target's size, shape, and materials. Additionally, the

UL APs are assumed to employ clutter rejection techniques to minimize interference from reflected clutter in the surrounding environment[57].

As the APs are connected to the CUP via the backhaul links, it is assumed that the direct-link interference (DLI), i.e., inter-AP interference, is known at the UL APs. Thus, the UL APs remove DLI before applying the sensing combiner, $\mathbf{u}_{nt} \in \mathbb{C}^{L\times 1}$ to process the sensing information from the t-th target. The post-processed signal for obtaining the t-th target's sensing information at the n-th UL AP is given as

$$\begin{aligned} y_{nt} &= \mathbf{u}_{nt}^H \left(\mathbf{y}_n - \sum_{m=1}^{M} \mathbf{F}_{mn} \mathbf{x}_m \right) \\ &= \underbrace{\alpha_t \mathbf{u}_{n\cdot t}^H \mathbf{g}_{n\cdot t}^{\mathrm{u}} \sum_{m=1}^{M} \left(\mathbf{g}_{m\cdot t}^{\mathrm{d}}\right)^H \left(\sum_{i=1}^{K} \mathbf{w}_{m\cdot i} q_i + \sum_{l=1}^{T} \mathbf{s}_{m\cdot l} \right)}_{t\text{-th target's desired reflection}} \\ &\quad + \underbrace{\sum_{j\neq t}^{T} \alpha_j \mathbf{u}_{n\cdot t}^H \mathbf{g}_{n\cdot j}^{\mathrm{u}} \sum_{m=1}^{M} \left(\mathbf{g}_{m\cdot j}^{\mathrm{d}}\right)^H \left(\sum_{i=1}^{K} \mathbf{w}_{m\cdot i} q_i + \sum_{j=1}^{T} \mathbf{s}_{m\cdot j} \right)}_{\text{Multi-target interference reflections}} \\ &\quad + \mathbf{u}_{nt}^H \mathbf{z}_n. \end{aligned} \tag{16}$$

C. Communication SE

From (14), communication SINR of the k-th user is obtained as

$$\mathrm{SINR}_k^{\mathrm{Com}} = \frac{\mathrm{DS}_k}{\sum_{i\neq k}^{K} \mathrm{MUI}_{ki} + \sum_{t=1}^{T} \mathrm{SSI}_{kt} + \sigma^2}, \tag{17}$$

where

$$\mathrm{DS}_k = \mathbb{E}\left\{ \left| \sum_{m=1}^{M} \mathbf{h}_{mk}^H \mathbf{w}_{mk} \right|^2 \right\}, \tag{18a}$$

$$\mathrm{MUI}_{ki} = \mathbb{E}\left\{ \left| \sum_{m=1}^{M} \mathbf{h}_{mk}^H \mathbf{w}_{mi} \right|^2 \right\}, \tag{18b}$$

$$\mathrm{SSI}_{kt} = \mathbb{E}\left\{ \left| \sum_{m=1}^{M} \mathbf{h}_{mk}^H \mathbf{s}_{mt} \right|^2 \right\}. \tag{18c}$$

To derive the closed-form solution, it is assumed that the DL APs adopt MRT beamforming for both communication and sensing, i.e., $\mathbf{w}_{mk} = \mathbf{h}_{mk}$ and $\mathbf{s}_{mt} = \mathbf{g}_{mt}^{\mathrm{d}}$. To this end, by evaluating the expectation terms in (17), the closed-form solution of the SINR at the k-th user is given in (19).

$$\mathrm{SINR}_k^{\mathrm{Com}} = \frac{L(L+1)\sum_{m=1}^{M} \zeta_{\mathbf{h}_{mk}}^2 + L^2 \sum_{m=1}^{M} \sum_{m'\neq m}^{M} \zeta_{\mathbf{h}_{mk}} \zeta_{\mathbf{h}_{m'k}}}{L\sum_{i\neq k}^{K} \sum_{m=1}^{M} \zeta_{\mathbf{h}_{mk}} \zeta_{\mathbf{h}_{mi}} + L\sum_{t=1}^{T} \sum_{m=1}^{M} \zeta_{\mathbf{h}_{mk}} \zeta_{\mathbf{g}_{mt}^{\mathrm{d}}} + \sigma^2} \tag{19}$$

Thus, the SE of the k-th user is given as

$$\mathcal{S}_k^{\mathrm{Com}} = \log_2\left(1 + \mathrm{SINR}_k^{\mathrm{Com}}\right). \tag{20}$$

D. Sensing SE

The sensing SE is used to evaluate sensing performance (Section III-C1). The UL APs perform the sensing, utilizing the targets' echoes. From (16), the sensing SE of the t-th target at the n-th UL AP is obtained as

$$\mathcal{S}_{nt}^{\mathrm{Sen}} \approx \log_2\left(1 + \mathrm{SINR}_{nt}^{\mathrm{Sen}}\right), \tag{21}$$

where the t-th target's sensing SINR an the n-th UL AP is given as

$$\mathrm{SINR}_{nt}^{\mathrm{Sen}} = \frac{|\alpha_t|^2 \mathrm{TDS}_{nt}}{\sum_{j\neq t}^{T} |\alpha_j|^2 \mathrm{MTI}_{n,tj} + \sigma^2 \mathbb{E}\{\|\mathbf{u}_{nt}\|^2\}}, \tag{22}$$

doi.org/10.32388/8SSIYA

where

$$\mathrm{TDS}_{nt} = \mathbb{E}\left\{\left|\mathbf{u}_{nt}^H \mathbf{g}_{nt}^{\mathrm{u}} \sum_{m=1}^{M} \mathbf{g}_{mt}^{\mathrm{d}H} \left(\sum_{i=1}^{K} \mathbf{w}_{mi} + \sum_{l=1}^{T} \mathbf{s}_{ml}\right)\right|^2\right\}, \tag{23a}$$

$$\mathrm{MTI}_{n,tj} = \mathbb{E}\left\{\left|\mathbf{u}_{nt}^H \mathbf{g}_{nj}^{\mathrm{u}} \sum_{m=1}^{M} \mathbf{g}_{mj}^{\mathrm{d}H} \left(\sum_{i=1}^{K} \mathbf{w}_{mi} + \sum_{j=1}^{T} \mathbf{s}_{mj}\right)\right|^2\right\}. \tag{23b}$$

By assuming the n-th UL AP employ the MRC to extract the t-th target's state information, i.e., $\mathbf{u}_{nt} = \mathbf{g}_{nt}^{\mathrm{u}}$, the closed-form expression of the sensing SINR, $\mathrm{SINR}_{nt}^{\mathrm{Sen}}$, is given in (24).

$$\mathrm{SINR}_{nt}^{\mathrm{Sen}} = \frac{|\alpha_t|^2 L(L+1)\zeta_{\mathbf{g}_{nt}^{\mathrm{u}}}^2 \sum_{m=1}^{M} \left(L\sum_{i=1}^{K} \zeta_{\mathbf{g}_{mt}^{\mathrm{d}}} \zeta_{\mathbf{h}_{mi}} + L(L+1)\zeta_{\mathbf{g}_{mt}^{\mathrm{d}}}^2 + L^2 \sum_{m' \neq m}^{M} \zeta_{\mathbf{g}_{mt}^{\mathrm{d}}} \zeta_{\mathbf{g}_{m't}^{\mathrm{d}}} + L\sum_{l \neq t}^{T} \zeta_{\mathbf{g}_{mt}^{\mathrm{d}}} \zeta_{\mathbf{g}_{ml}^{\mathrm{d}}}\right)}{\sum_{j \neq t}^{T} |\alpha_j|^2 L \zeta_{\mathbf{g}_{nt}^{\mathrm{u}}} \zeta_{\mathbf{g}_{nj}^{\mathrm{u}}} \sum_{m=1}^{M} \left(L\sum_{i=1}^{K} \zeta_{\mathbf{g}_{mt}^{\mathrm{d}}} \zeta_{\mathbf{h}_{mi}} + L(L+1)\zeta_{\mathbf{g}_{mj}^{\mathrm{d}}}^2 + L^2 \sum_{m' \neq m}^{M} \zeta_{\mathbf{g}_{mj}^{\mathrm{d}}} \zeta_{\mathbf{g}_{m'j}^{\mathrm{d}}} + L\sum_{l \neq t}^{T} \zeta_{\mathbf{g}_{mj}^{\mathrm{d}}} \zeta_{\mathbf{g}_{ml}^{\mathrm{d}}}\right) + L\sigma^2 \zeta_{\mathbf{g}_{nt}^{\mathrm{u}}}} \tag{24}$$

Footnotes

[1] Throughout this paper, "system-/link-level ISAC" is used interchangeably with "conventional ISAC".

References

1. a, b, c, d, e, f, g, h, i, j *Liu A, Huang Z, Li M, Wan Y, Li W, Han TX, Liu C, Du R, Tan DKP, Lu J, Shen Y, Colone F, Chetty K (2022). "A Survey on Fundamental Limits of Integrated Sensing and Communication." IEEE Commun. Surveys Tuts.. **24** (2): 994–1034. doi:10.1109/COMST.2022.3149272.*
2. a, b, c, d, e, f, g, h, i *Wang J, Varshney N, Gentile C, Blandino S, Chuang J, Golmie N (2022). "Integrated Sensing and Communication: Enabling Techniques, Applications, Tools and Data Sets, Standardization, and Future Directions." IEEE Internet Things J. **9** (23): 23416–23440. doi:10.1109/JIOT.2022.3190845.*
3. a, b, c, d, e, f, g, h *Zhang JA, Rahman ML, Wu K, Huang X, Guo YJ, Chen S, Yuan J (2022). "Enabling Joint Communication and Radar Sensing in Mobile Networks — A Survey." IEEE Commun. Surveys Tuts.. **24** (1): 306–345. doi:10.1109/COMST.2021.3122519.*
4. a, b, c, d, e, f, g, h, i, j, k, l *Hakimi A, Galappaththige D, Tellambura C (2024). "A roadmap for NF-ISAC in 6G: A comprehensive overview and tutorial." Entropy. **26** (9): 773. doi:10.3390/e26090773.*
5. a, b, c, d, e, f, g, h, i, j, k, l, m, n, o, p, q, r, s, t, u, v, w, x, y, z, Α, Β, Γ *Liu F, Masouros C, Eldar Y, editors. Integrated Sensing and Communications. Singapore: Springer Singapore; 2023 Jul 20. doi:10.1007/978-981-99-2501-8.*
6. a, b, c, d, e, f, g, h, i, j, k, l, m, n, o *Mao W, Lu Y, Liu J, Ai B, Zhong Z, Ding Z (2023). "Beamforming Design in Cell-Free Massive MIMO Integrated Sensing and Communication Systems." In: Proc. IEEE Global Commun. Conf., Dec. 2023, pp. 546–551. doi:10.1109/GLOBECOM54140.2023.10437290.*
7. a, b, c, d, e, f, g, h, i, j, k, l, m, n, o *Demirhan U, Alkhateeb A (2023). "Cell-Free Joint Sensing and Communication MIMO: A Max-Min Fair Beamforming Approach." In: Proc. IEEE Asilomar Conf. Signals, Syst., Comput.. pp. 381–386. doi:10.1109/IEEECONF59524.2023.10477011.*
8. a, b, c, d, e, f, g, h, i, j, k, l, m, n *Huang Y, Fang Y, Li X, Xu J (2022). "Coordinated Power Control for Network Integrated Sensing and Communication". IEEE Trans. Veh. Technol.. **71** (12): 13361–13365. doi:10.1109/TVT.2022.3194139.*
9. a, b, c, d, e, f, g, h, i, j, k, l, m, n, o *Cao Y, Yu QY. "Design and performance analyses of V-OFDM integrated signal for cell-free massive MIMO joint communication and radar system." IEEE Syst. J.. **17**(4): 5943–5954, Dec. 2023. doi:10.1109/JSYST.2023.3301490.*
10. a, b, c, d, e, f, g, h, i, j *Wang B, Xu L, Cheng Z, He Z (2023). "Semi-Distributed Hybrid Beamforming Design for Cooperative Cell-Free Dual-Function Radar-Communication Networks." In: Proc. IEEE Int. Conf. Acoust., Speech, Signal Process. Workshops. Jun. 2023, pp. 1-5. doi:10.1109/ICASSPW59220.2023.10193721.*
11. a, b, c, d, e, f, g, h, i *Sakhnini A, Bourdoux A, Guenach M, Sahli H, Pollin S. "Uplink Payload Power Control in Cell-Free Communication and Radar Networks." In: Proc. IEEE Global Commun. Conf., Dec. 2022, pp. 5111-5116. doi:10.1109/GLOBECOM48099.2022.10001650.*

12. ^ a b c d e f g h i j *Da Silva IW, Osorio DP, Juntti M. "Multi-Static ISAC in Cell-Free Massive MIMO: Precoder Design and Privacy Assessment." In: Proc. IEEE Globecom Workshops, Dec. 2023, pp. 461-466. doi:10.1109/GCWkshps58843.2023.10465106.*

13. ^ a b c d e f g h i *Behdad Z, Demir {\"O}T, Sung KW, Bj{\"o}rnson E, Cavdar C. "Power Allocation for Joint Communication and Sensing in Cell-Free Massive MIMO." In: Proc. IEEE Global Commun. Conf.; 2022 Dec. p. 4081-4086. doi:10.1109/GLOBECOM48099.2022.10000730.*

14. ^ a b c d e f g h i j k l m *Behdad Z, Demir {\"O}T, Sung KW, Cavdar C (2024). "Interplay Between Sensing and Communication in Cell-Free Massive MIMO with URLLC Users." In: Proc. IEEE Wireless Commun. Netw. Conf., Apr. 2024, pp. 1-6. doi:10.1109/WCNC57260.2024.10571226.*

15. ^ *Gesbert D, Hanly S, Huang H, Shamai Shitz S, Simeone O, Yu W (2010). "Multi-Cell MIMO Cooperative Networks: A New Look at Interference." IEEE J Sel Areas Commun. **28** (9): 1380–1408. doi:10.1109/JSAC.2010.101202.*

16. ^ *Dahrouj H, Yu W (2010). "Coordinated beamforming for the multicell multi-antenna wireless system". IEEE Trans. Wireless Commun.. **9** (5): 1748–1759. doi:10.1109/TWC.2010.05.090936.*

17. ^ *Wu J, Zhang Z, Hong Y, Wen Y (2015). "Cloud radio access network (C-RAN): A primer". IEEE Netw.. **29** (1): 35-41. doi:10.1109/MNET.2015.7018201.*

18. ^ a b c d e f g h i j k l m n o p q r s t u v w x y z ^ ^ ^ *Ngo HQ, Ashikhmin A, Yang H, Larsson EG, Marzetta TL (2017). "Cell-Free Massive MIMO Versus Small Cells". IEEE Trans. Wireless Commun.. **16** (3): 1834–1850. doi:10.1109/TWC.2017.2655515.*

19. ^ *Fishler E, Haimovich A, Blum R, Chizhik D, Cimini L, Valenzuela R (2004). "MIMO radar: An idea whose time has come." In: Proc. IEEE Radar Conf.. Aug. 2004. pp. 71-78. doi:10.1109/NRC.2004.1316398.*

20. ^ a b c *Haimovich AM, Blum RS, Cimini LJ (2008). "MIMO Radar with Widely Separated Antennas". IEEE Signal Process. Mag.. **25** (1): 116-129. doi:10.1109/MSP.2008.4408448.*

21. ^ a b c d e f *Richards MA. Fundamentals Of Radar Signal Processing. McGraw-Hill Education (India) Pvt Limited; 2005. ISBN **9780070607378**.*

22. ^ a b c d e f g h i j k l m n o p q r s t u v w x y z ^ *Demir ÖT, Björnson E, Sanguinetti L. Foundations of User-Centric Cell-Free Massive MIMO. Foundations and trends in signal processing. Now Publishers; 2021. ISBN 9781680837902.*

23. ^ a b c *Ammar HA, Adve R, Shahbazpanahi S, Boudreau G, Srinivas KV (2022). "User-Centric Cell-Free Massive MIMO Networks: A Survey of Opportunities, Challenges and Solutions." IEEE Commun. Surveys Tuts.. **24** (1): 611–652. doi:10.1109/COMST.2021.3135119.*

24. ^ *Interdonato G, Bjf6rnson E, Ngo HQ, Frenger PK, Larsson EG (2019). "Ubiquitous Cell-Free Massive MIMO Communications". EURASIP J. Wireless Commun. Netw.. **2019**: 1687-1499. doi:10.1186/s13638-019-1507-0.*

25. ^ *Zhang J, Bjf6rnson E, Matthaiou M, Ng DWK, Yang H, Love DJ (2020). "Prospective Multiple Antenna Technologies for Beyond 5G". IEEE J. Sel. Areas Commun.. **38** (8): 1637–1660. doi:10.1109/JSAC.2020.3000826.*

26. ^ a b *Elhoushy S, Ibrahim M, Hamouda W (2022). "Cell-free massive MIMO: A survey". IEEE Commun. Surveys Tuts.. **24** (1): 492–523. doi:10.1109/COMST.2021.3123267.*

27. ^ a b c d e f g h i j k l m n o p q r s t u v w x y z ^ ^ ^ ^ ^ ^ ^ *Zhang J, Chen S, Lin Y, Zheng J, Ai B, Hanzo L (2019). "Cell-Free Massive MIMO: A New Next-Generation Paradigm". IEEE Access. **7**: 99878–99888. doi:10.1109/ACCESS.2019.2930208.*

28. ^ *Chen S, Zhang J, Zhang J, Bjf6rnson E, Ai B. "A survey on user-centric cell-free massive MIMO systems." Digital Commun. Netw.. **8**(5): 695-719, Dec. 2022. doi:10.1016/j.dcan.2021.12.005.*

29. ^ *Kassam J, Castanheira D, Silva A, Dinis R, Gameiro A (2023). "A review on cell-free massive MIMO systems." Electronics. **12**(4): 1001. doi:10.3390/electronics12041001.*

30. ^ *Mohammadi M, Mobini Z, Quoc Ngo H, Matthaiou M (2024). "Next-Generation Multiple Access With Cell-Free Massive MIMO". Proc. IEEE. **112** (9): 1372–1420. doi:10.1109/JPROC.2024.3451372.*

31. ^ a b *Galappaththige D, Amarasuriya G (2019). "Cell-Free Massive MIMO with Underlay Spectrum-Sharing." In: Proc. IEEE Int. Conf. Commun.. May 2019, pp. 1-7. doi:10.1109/ICC.2019.8761777.*

32. ^ a b *Galappaththige D, Shrestha R, Aruma Baduge GA (2021). "Exploiting Cell-Free Massive MIMO for Enabling Simultaneous Wireless Informati on and Power Transfer". IEEE Trans. Green Commun. Netw.. **5** (3): 1541–1557. doi:10.1109/TGCN.2021.3090357.*

33. ^ a b *Galappaththige D, Amarasuriya G (2020). "NOMA-Aided Cell-Free Massive MIMO with Underlay Spectrum-Sharing." In: Proc. IEEE Int. Conf. Commun.. pp. 1-6. doi:10.1109/ICC40277.2020.9149105.*

34. ^ a b *Galappaththige D, Tellambura C (2024). "Sum Rate Maximization for RSMA-Assisted CF mMIMO Networks With SWIPT Users." IEEE Wirele ss Commun. Lett.. **13** (5): 1300-1304. doi:10.1109/LWC.2024.3368272.*

35. ^ a b *Galappaththige D, Kudathanthirige D, Amarasuriya G. "Performance Analysis of {IRS}-Assisted Cell-Free Communication." In: Proc. IEEE Gl obal Commun. Conf., Dec. 2021, pp. 1-6. doi:10.1109/GLOBECOM46510.2021.9685730.*

36. ^ a b *Galappaththige D, Baduge GAA (2021). "Exploiting Underlay Spectrum Sharing in Cell-Free Massive MIMO Systems." IEEE Trans Commun. **69** (11): 7470–7488. doi:10.1109/TCOMM.2021.3088517.*

37. ^ *Bjf6rnson E, Hoydis J, Sanguinetti L. Massive MIMO Networks: Spectral, Energy, and Hardware Efficiency. 2017. Vol. 11. pp. 154⊠655.*

38. ^ *Marzetta TL, Larsson EG, Yang H, Ngo HQ. Fundamentals of Massive MIMO. Cambridge: Cambridge University Press; 2016. doi:10.1017/CBO978 1316799895.*

39. ^ *Ngo HQ, Tran L-N, Duong TQ, Matthaiou M, Larsson EG. "On the Total Energy Efficiency of Cell-Free Massive MIMO." IEEE Trans. Green Com mu. and Networking. **2**(1): 25-39, Mar. 2018. doi:10.1109/TGCN.2017.2770215.*

40. ^ a b *Galappaththige D, Rezaei F, Tellambura C, Maaref A (2024). "Cell-Free Bistatic Backscatter Communication: Channel Estimation, Optimizati on, and Performance Analysis". IEEE Trans. Commun.. **72** (10): 6617–6632. doi:10.1109/TCOMM.2024.3402615.*

41. ^ a b *Bjf6rnson E, Sanguinetti L (2020). "Scalable Cell-Free Massive MIMO Systems". IEEE Trans. Commun.. **68** (7): 4247-4261. doi:10.1109/TCOM M.2020.2987311.*

42. ^ *Parida P, Dhillon HS (2023). "Cell-Free Massive MIMO With Finite Fronthaul Capacity: A Stochastic Geometry Perspective". IEEE Trans. Wirele ss Commun.. **22** (3): 1555–1572. doi:10.1109/TWC.2022.3205349.*

43. ^ *Elhoshy S, Ibrahim M, Ashour M, Elshabrawy T, Hammad H, Rizk MRM. "A dimensioning framework for indoor DAS LTE networks." In: Proc. I nt. Conf. Sel. Topics Mobile Wireless Netw.; 2016 Apr. p. 1-8. doi:10.1109/MoWNet.2016.7496616.*

44. ^ *Irmer R, Droste H, Marsch P, Grieger M, Fettweis G, Brueck S, Mayer HP, Thiele L, Jungnickel V (2011). "Coordinated multipoint: Concepts, perfor mance, and field trial results." IEEE Commun. Mag. **49** (2): 102-111. doi:10.1109/MCOM.2011.5706317.*

45. ^ *Venkatesan S, Lozano A, Valenzuela R. "Network MIMO: Overcoming Intercell Interference in Indoor Wireless Systems." In: Proc. IEEE Asiloma r Conf. Signals, Syst., Comput.; 2007 Nov. p. 83-87. doi:10.1109/ACSSC.2007.4487170.*

46. ^ *Simeone O, Somekh O, Vincent Poor H, Shamai S. "Distributed MIMO in multi-cell wireless systems via finite-capacity links." In: Proc. 3rd Int. S ymp. Commun., Control Signal Process.; 2008 Mar. p. 203-206. doi:10.1109/ISCCSP.2008.4537220.*

47. ^ ***Intel Corporation** (2021). "Exploring 5G Fronthaul Network Architecture: Intelligence Splits and Connectivity." Intel Corporation, Tech. Rep. [O nline]. Available: https://www.intel.com/content/dam/www/public/us/en/documents/white-papers/exploring-5g-fronthaul-network-architect ure-white-paper.pdf.*

48. ^ *Peng M, Li Y, Zhao Z, Wang C (2015). "System architecture and key technologies for 5G heterogeneous cloud radio access networks". IEEE Net w.. **29** (2): 6–14. doi:10.1109/MNET.2015.7064897.*

49. ^ *Mao Y, You C, Zhang J, Huang K, Letaief KB. "A Survey on Mobile Edge Computing: The Communication Perspective." IEEE Commun. Surveys Tuts.. **19** (4): 2322–2358, 4th Quart. 2017. doi:10.1109/COMST.2017.2745201.*

50. ^ a b c d e f *Chen Z, Björnson E. "Channel Hardening and Favorable Propagation in Cell-Free Massive MIMO With Stochastic Geometry." IEEE Tr ans. Commun. **66** (11): 5205-5219, Nov. 2018. doi:10.1109/TCOMM.2018.2846272.*

51. ^ a b c d e f *Polegre AA, Riera-Palou F, Femenias G, Armada AG (2020). "Channel Hardening in Cell-Free and User-Centric Massive MIMO Networ ks With Spatially Correlated Ricean Fading." IEEE Access. **8**: 139827–139845. doi:10.1109/ACCESS.2020.3012736.*

52. ^ *Papoulis A, Pillai SU. Probability, Random Variables, and Stochastic Processes. McGraw-Hill series in electrical and computer engineering. Mc Graw-Hill; 2002. ISBN 97800712266l5. LCCN 2001044139.*

53. a, b, c, d, e, f, g, h, i *Mao W, Lu Y, Chi CY, Ai B, Zhong Z, Ding Z (2024). "Communication-Sensing Region for Cell-Free Massive MIMO ISAC Systems". IEEE Trans. Wireless Commun.. doi:10.1109/TWC.2024.3392330.*

54. a, b *Ngo HQ, Tran L-N, Duong TQ, Matthaiou M, Larsson EG. "Energy efficiency optimization for cell-free massive MIMO." In: Proc. IEEE Int. Wor kshop Signal Process. Adv. Wireless Commun.; 2017 Jul. p. 1-5. doi:10.1109/SPAWC.2017.8227722.*

55. ^ *Papazafeiropoulos A, Kourtessis P, Renzo MD, Chatzinotas S, Senior JM (2020). "Performance Analysis of Cell-Free Massive MIMO Systems: A Stochastic Geometry Approach". IEEE Trans. Veh. Technol.. **69** (4): 3523–3537. doi:10.1109/TVT.2020.2970018.*

56. a, b *Yang H, Marzetta TL. "Energy Efficiency of Massive MIMO: Cell-Free vs. Cellular." In: Proc. IEEE 87th Veh. Technol. Conf., Jun. 2018, pp. 1-5. do i:10.1109/VTCSpring.2018.8417645.*

57. a, b, c, d, e, f, g, h, i, j, k, l, m, n, o, p, q, r, s, t, u, v, w, x, y, z, ^ *Richards MA, Scheer JA, Holm WA, editors. Principles of Mo dern Radar: Basic principles. Radar, Sonar and Navigation. Institution of Engineering and Technology; 2010.*

58. ^ *Knott EF, Schaeffer JF, Tulley MT. Radar Cross Section. Radar, Sonar and Navigation Series. Institution of Engineering and Technology; 2004. I SBN 9781891121258. LCCN 2006355105.*

59. ^ *Rezende MC, Martin IM, Miacci MAS, Nohara EL. "Radar Cross Section Measurements (8-12 GHz) of Magnetic and Dielectric Microwave Absor bing Thin Sheets." In: Proc. SBMO/IEEE MTT-S Int. Microw. Optoelectronics Conf., Dec. 2002, pp. 439-443. doi:10.1109/IMOC.2001.942566.*

60. ^ *Skolnik MI. Introduction to Radar Systems. Electrical engineering series. McGraw-Hill; 2001. ISBN 9780071181891. LCCN 79015354.*

61. ^ *Sayama S, Sekine H (2001). "Weibull, log-Weibull and K-distributed ground clutter modeling analyzed by AIC." IEEE Trans. Aerosp. Electron. S yst.. **37** (3): 1108-1113. doi:10.1109/7953262.*

62. a, b *Levanon N, Mozeson E. Radar Signals. IEEE Press. Wiley; 2004. ISBN **9780471663072**.*

63. a, b *Blunt SD, Mokole EL (2016). "Overview of radar waveform diversity". IEEE Aerosp. Electron. Syst. Mag.. **31** (11): 2–42. doi:10.1109/MAES.2016.1 60071.*

64. ^ *Li J, Li J, Stoica P. MIMO Radar Signal Processing. IEEE Press. Wiley; 2009. ISBN 9780470178980. LCCN 2008022134.*

65. ^ *Mohammadi M, Mobini Z, Galappaththige D, Tellambura C (2023). "A Comprehensive Survey on Full-Duplex Communication: Current Solutio ns, Future Trends, and Open Issues". IEEE Commun. Surveys Tuts.. 2nd Quart. 2023: 1–1. doi:10.1109/COMST.2023.3318198.*

66. ^ *Galappaththige D, Mohammadi M, Ngo HQ, Matthaiou M, Tellambura C (2024). "Cell-Free Full-Duplex Communication -- An Overview". arXi v. eprint:2412.04711.*

67. ^ *Xiong Y, Liu F, Cui Y, Yuan W, Han TX. "Flowing the Information from Shannon to Fisher: Towards the Fundamental Tradeoff in ISAC." In: Proc. IEEE Global Commun. Conf.; 2022 Dec. p. 5601-5606. doi:10.1109/GLOBECOM48099.2022.10001144.*

68. a, b *Ma D, Shlezinger N, Huang T, Liu Y, Eldar YC (2020). "Joint Radar-Communication Strategies for Autonomous Vehicles: Combining Two Key Automotive Technologies". IEEE Signal Process. Mag.. **37** (4): 85-97. doi:10.1109/MSP.2020.2983832.*

69. ^ *Ma D, Shlezinger N, Huang T, Liu Y, Eldar YC (2021). "FRaC: FMCW-Based Joint Radar-Communications System via Index Modulation." IEEE J. Sel. Topics Signal Process.. **15** (6): 1348–1364. doi:10.1109/JSTSP.2021.3118219.*

70. a, b *Chen L, Wang Z, Du Y, Chen Y, Yu FR (2022). "Generalized Transceiver Beamforming for DFRC with MIMO Radar and MU-MIMO Communic ation". IEEE J. Sel. Areas Commun.. **40** (6): 1795–1808. doi:10.1109/JSAC.2022.3155515.*

71. a, b *Liu X, Huang T, Shlezinger N, Liu Y, Zhou J, Eldar YC (2020). "Joint Transmit Beamforming for Multiuser MIMO Communications and MIMO Radar". IEEE Trans. Signal Process.. **68**: 3929–3944. doi:10.1109/TSP.2020.3004739.*

72. a, b, c, d *Bell MR (1993). "Information theory and radar waveform design." IEEE Trans. Inf. Theory. **39** (5): 1578–1597. doi:10.1109/18.259642.*

73. a, b, c, d *Tang B, Tang J, Peng Y (2010). "MIMO Radar Waveform Design in Colored Noise Based on Information Theory". IEEE Trans. Signal Proce ss.. **58** (9): 4684–4697. doi:10.1109/TSP.2010.2050885.*

74. a, b, c, d, eZhang JA, Liu F, Masouros C, Heath RW, Feng Z, Zheng L, Petropulu A (2021). "An Overview of Signal Processing Techniques for Joint Communication and Radar Sensing." IEEE J Sel Topics Signal Process. **15**(6): 1295–1315. doi:10.1109/JSTSP.2021.3113120.

75. a, b, c, d, e, f, g, hKay SM. Fundamentals of Statistical Signal Processing, Vol. I: Estimation Theory. Englewood Cliffs, NJ, USA: Prentice Hall; 1998.

76. a, b, c, d, e, f, gHe Z, Xu W, Shen H, Huang Y, Xiao H (2022). "Energy Efficient Beamforming Optimization for Integrated Sensing and Communication". IEEE Wireless Commun. Lett.. **11** (7): 1374–1378. doi:10.1109/LWC.2022.3169517.

77. a, b, c, dStoica P, Li J, Xie Y (2007). "On probing signal design for MIMO radar". IEEE Trans. Signal Process.. **55** (8): 4151–4161. doi:10.1109/TSP.2007.894398.

78. a, b, c, d, e, f, g, h, i, jCui G, Li H, Rangaswamy M (2014). "MIMO Radar Waveform Design With Constant Modulus and Similarity Constraints". IEEE Trans. Signal Process.. **62** (2): 343–353. doi:10.1109/TSP.2013.2288086.

79. a, b, c, dHua H, Xu J, Han TX (2023). "Optimal Transmit Beamforming for Integrated Sensing and Communication". IEEE Transactions on Vehicular Technology. **72** (8): 10588–10603. doi:10.1109/TVT.2023.3262513.

80. a, b, c, d, e, f, g, hTang B, Li J (2019). "Spectrally constrained MIMO radar waveform design based on mutual information." IEEE Trans. Signal Process. **67** (3): 821–834. doi:10.1109/TSP.2018.2887186.

81. a, b, c, d, e, f, g, h, i, j, kHe Z, Xu W, Shen H, Ng DWK, Eldar YC, You X (2023). "Full-Duplex Communication for ISAC: Joint Beamforming and Power Optimization." IEEE J. Sel. Areas Commun.. **41** (9): 2920–2936. doi:10.1109/JSAC.2023.3287540.

82. a, b, c, d, eOuyang C, Liu Y, Yang H (2022). "Performance of Downlink and Uplink Integrated Sensing and Communications (ISAC) Systems". IEEE Wireless Commun. Lett.. **11** (9): 1850–1854. doi:10.1109/LWC.2022.3184409.

83. a, bGalappaththige D, Tellambura C, Maaref A (2023). "Integrated Sensing and Backscatter Communication". IEEE Wireless Commun. Lett.. **12** (12): 2043–2047. doi:10.1109/LWC.2023.3305981.

84. ^Bekkerman I, Tabrikian J (2006). "Target Detection and Localization Using MIMO Radars and Sonars." IEEE Trans. Signal Process.. **54** (10): 3873–3883. doi:10.1109/TSP.2006.879267.

85. ^Dan Q, Lei H, Park K-H, Pan G, Alouini M-S (2024). "Beamforming Design for Joint Target Sensing and Proactive Eavesdropping". arXiv. Available from: https://arxiv.org/abs/2407.06521.

86. a, bLi J, Stoica P (2007). "MIMO Radar with Colocated Antennas". IEEE Signal Process. Mag.. **24** (5): 106–114. doi:10.1109/MSP.2007.904812.

87. a, bLiu F, Masouros C, Petropulu AP, Griffiths H, Hanzo L (2020). "Joint Radar and Communication Design: Applications, State-of-the-Art, and the Road Ahead." IEEE Trans. Commun.. **68** (6): 3834–3862. doi:10.1109/TCOMM.2020.2973976.

88. a, b, c, dRivetti S, Björnson E, Skoglund M. "Secure Spatial Signal Design for ISAC in a Cell-Free MIMO Network." In: Proc. IEEE Wireless Commun. Netw. Conf., Apr. 2024, pp. 01–06. doi:10.1109/WCNC57260.2024.10570706.

89. ^Galappaththige D, Zargari S, Tellambura C, Li GY (2025). "Optimization of Rate-Splitting Multiple Access With Integrated Sensing and Backscatter Communication". IEEE Trans. Veh. Technol.. pp. 1–16. doi:10.1109/TVT.2025.3536330.

90. ^Zargari S, Galappaththige D, Tellambura C (2025). "Transmit Power-Efficient Beamforming Design for Integrated Sensing and Backscatter Communication". IEEE Open J. Commun. Soc.. pp. 1–1. doi:10.1109/OJCOMS.2025.3527860.

91. a, b, c, d, e, f, g, h, i, jZargari S, Galappaththige D, Tellambura C, Li GY (2024). "Downlink Beamforming for Cell-Free ISAC: A Fast Complex Oblique Manifold Approach". arXiv. eprint:2409.06847.

92. a, b, cZeng T, Semiari O, Saad W, Bennis M (2019). "Joint Communication and Control for Wireless Autonomous Vehicular Platoon Systems". IEEE Trans. Commun.. **67** (11): 7907–7922. doi:10.1109/TCOMM.2019.2931583.

93. a, b, cMilanes V, Villagra J, Godoy J, Simo J, Perez J, Onieva E (2012). "An Intelligent V2I-Based Traffic Management System". IEEE Trans. Intell. Transp. Syst.. **13** (1): 49–58. doi:10.1109/TITS.2011.2178839.

94. a, b, cMa Y, Zhou G, Wang S (2019). "WiFi Sensing with Channel State Information: A Survey". ACM Comput. Surv.. **52** (3): 46. doi:10.1145/3310194.

95. ^ a b Popovski P, Stefanovic C, Nielsen JJ, de Carvalho E, Angjelichinoski M, Trillingsgaard KF, Bana A-S (2019). "Wireless Access in Ultra-Reliable Low-Latency Communication (URLLC)". IEEE Trans. Commun.. **67** (8): 5783–5801. doi:10.1109/TCOMM.2019.2914652.

96. ^ a b c Philip NY, Rodrigues JJP, Wang H, Fong SJ, Chen J (2021). "Internet of Things for In-Home Health Monitoring Systems: Current Advances, Challenges and Future Directions." IEEE J Sel Areas Commun. **39**(2): 300-310. doi:10.1109/JSAC.2020.3042421.

97. ^ a b Prakash C, Singh LP, Gupta A, Lohan SK (2023). "Advancements in smart farming: A comprehensive review of IoT, wireless communication, sensors, and hardware for agricultural automation." Sensors and Actuators A: Physical. **362**: 114605. doi:10.1016/j.sna.2023.114605.

98. ^ Zargari S, Galappaththige D, Tellambura C, Poor HV. "A Riemannian Manifold Approach to Constrained Resource Allocation in ISAC." IEEE Trans. Commun.. 2024: 1-1. doi:10.1109/TCOMM.2024.3487801.

99. ^ Rahman ML, Zhang JA, Huang X, Guo YJ, Heath RW (2020). "Framework for a perceptive mobile network using joint communication and radar sensing". IEEE Trans. Aerosp. Electron. Syst.. **56** (3): 1926–1941. doi:10.1109/TAES.2019.2939611.

100. ^ Galappaththige D, Zargari S, Tellambura C, Li GY (2024). "Near-Field ISAC: Beamforming for Multi-Target Detection". IEEE Wireless Commun. Lett.. **13** (7): 1938–1942. doi:10.1109/LWC.2024.3397081.

101. ^ Galappaththige D, Zargari S, Tellambura C, Li GY (2025). "Low-Complexity Multi-Target Detection in ELAA ISAC." IEEE Commun. Lett.. doi:10.1109/LCOMM.2025.3537457.

102. ^ Ouyang C, Liu Y, Yang H (2022). "On the performance of uplink ISAC systems." IEEE Commun. Lett.. **26**(8): 1769-1773. doi:10.1109/LCOMM.2022.3178193.

103. ^ Babu N, Masouros C, Papadias CB, Eldar YC (2024). "Precoding for Multi-Cell ISAC: From Coordinated Beamforming to Coordinated Multipoint and Bi-Static Sensing". IEEE Trans. Wireless Commun.. **23** (10): 14637–14651. doi:10.1109/TWC.2024.3417713.

104. ^ Wang Z, Xiao C, Liu X, Peng M, Guo J (2024). "Interference Mitigation in Multi-Cell ISAC Systems: A Three-Dimensional MIMO Precoding Approach". IEEE Commun. Lett.. **28** (11): 2543–2547. doi:10.1109/LCOMM.2024.3424194.

105. ^ a b Li R, Xiao Z, Zeng Y (2024). "Toward seamless sensing coverage for cellular multi-static integrated sensing and communication". IEEE Trans. Wireless Commun.. **23** (6): 5363–5376. doi:10.1109/TWC.2023.3325849.

106. ^ a b Meng K, Masouros C, Petropulu AP, Hanzo L (2024). "Cooperative ISAC Networks: Performance Analysis, Scaling Laws and Optimization". IEEE Trans. Wireless Commun.. doi:10.1109/TWC.2024.3491356.

107. ^ Meng K, Masouros C, Petropulu AP, Hanzo L (2024). "Cooperative ISAC Networks: Opportunities and Challenges." IEEE Wireless Commun.. pp. 1-8. doi:10.1109/MWC.008.2400151.

108. ^ Mohammadi M, Vu TT, Ngo HQ, Matthaiou M (2023). "Network-Assisted Full-Duplex Cell-Free Massive MIMO: Spectral and Energy Efficiencies". IEEE J. Sel. Areas Commun.. **41** (9): 2833–2851. doi:10.1109/JSAC.2023.3287613.

109. ^ Fishler E, Haimovich A, Blum RS, Cimini LJ, Chizhik D, Valenzuela RA (2006). "Spatial Diversity in Radars—Models and Detection Performance." IEEE Trans. Signal Process. **54** (3): 823–838. doi:10.1109/TSP.2005.862813.

110. ^ a b c d e f g Dong Y, Wang H, Yang Z, Hao N, Zhang C, Yu X (2024). "Cell-free ISAC massive MIMO systems with capacity-constrained fronthaul links". Digital Signal Processing. **145**: 104341. doi:10.1016/j.dsp.2023.104341.

111. ^ a b c d e f g h Demirhan U, Alkhateeb A (2024). "Cell-Free ISAC MIMO Systems: Joint Sensing and Communication Beamforming". arXiv. Available from: arXiv:2301.11328.

112. ^ a b c d e f g Elfiatoure M, Mohammadi M, Ngo HQ, Matthaiou M (2023). "Cell-Free Massive MIMO for ISAC: Access Point Operation Mode Selection and Power Control." In: Proc. IEEE Global Commun. Conf., Dec. 2023, pp. 104-109. doi:10.1109/GCWkshps58843.2023.10465053.

113. ^ a b c d e f g h Liu S, Liu R, Lu Z, Li M, Liu Q (2024). "Cooperative Cell-Free ISAC Networks: Joint BS Mode Selection and Beamforming Design." In: Proc. IEEE Wireless Commun. Netw. Conf., Apr. 2024, pp. 1-6. doi:10.1109/WCNC57260.2024.10571110.

114. ^ Elfiatoure M, Mohammadi M, Ngo HQ, Shin H, Matthaiou M (2025). "Multiple-Target Detection in Cell-Free Massive MIMO-Assisted ISAC". IEEE Trans. Wireless Commun..

115. ^Moerman A, Van Kerrebrouck J, Caytan O, de Paula IL, Bogaert L, Torfs G, Demeester P, Rogier H, Lemey S (2022). "Beyond 5G Without Obstacles: mmWave-over-Fiber Distributed Antenna Systems." IEEE Commun. Mag.. **60** (1): 27-33. doi:10.1109/MCOM.001.2100550.

116. ^You XH, Wang DM, Sheng B, Gao XQ, Zhao XS, Chen M (2010). "Cooperative distributed antenna systems for mobile communications [Coordinated and Distributed MIMO]". IEEE Wireless Commun.. **17** (3): 35-43. doi:10.1109/MWC.2010.5490977.

117. a, bSakhnini A, Guenach M, Bourdoux A, Sahli H, Pollin S. "A Target Detection Analysis in Cell-Free Massive MIMO Joint Communication and Radar Systems." In: Proc. IEEE Int. Conf. Commun.; May 2022. p. 2567-2572. doi:10.1109/ICC45855.2022.9838883.

118. a, bBehdad Z, Demir {\"O}T, Sung KW, Bj\u00f6rnson E, Cavdar C (2024). "Multi-Static Target Detection and Power Allocation for Integrated Sensing and Communication in Cell-Free Massive MIMO". IEEE Trans. Wireless Commun.. doi:10.1109/TWC.2024.3383209.

119. a, bKulathunga R, Dassanayake J, Amarasuriya G. "Cell-Free Massive MIMO-Aided ISAC." In: Proc. IEEE Int. Conf. Commun., Montreal, Quebec, Canada, Jun. 2025, pp. 1-6, accepted.

120. ^3GPP TR 36.814, Further Advancements for E-UTRA Physical Layer Aspects, V9.0.0 Rel. 9. Mar. 2010. Available Online: https://portal.3gpp.org/desktopmodules/Specifications/SpecificationDetails.aspx?specificationId=2493.

121. a, bBehdad Z, Demir {\"O}T, Sung KW, Cavdar C (2024). "Joint Processing and Transmission Energy Optimization for ISAC in Cell-Free Massive MIMO with URLLC". arXiv. Available from: arXiv:2401.10315.

122. ^Qu K, Ye J, Li X, Guo S (2024). "Privacy and Security in Ubiquitous Integrated Sensing and Communication: Threats, Challenges and Future Directions". IEEE Internet Things Mag.. **7** (4): 52-58. doi:10.1109/IOTM.001.2300180.

123. ^Zhu X, Liu J, Lu L, Zhang T, Qiu T, Wang C, Liu Y (2024). "Enabling Intelligent Connectivity: A Survey of Secure ISAC in 6G Networks". IEEE Commun. Surveys Tuts.. doi:10.1109/COMST.2024.3432871.

124. a, bNasir AA (2024). "Joint Users' Secrecy Rate and Target's Sensing SNR Maximization for a Secure Cell-Free ISAC System." IEEE Commun. Lett.. **28** (7): 1549–1553. doi:10.1109/LCOMM.2024.3406398.

125. a, bRen Z, Xu J, Qiu L, Ng DWK (2024). "Secure Cell-Free Integrated Sensing and Communication in the Presence of Information and Sensing Eavesdroppers". IEEE J. Sel. Areas Commun.. doi:10.1109/JSAC.2024.3431582.

126. ^Cao Y, Yu QY (2023). "Joint Resource Allocation for User-Centric Cell-Free Integrated Sensing and Communication Systems". IEEE Commun. Lett.. **27** (9): 2338–2342. doi:10.1109/LCOMM.2023.3301535.

127. a, b, cBuzzi S, D'Andrea C, Liesegang S. "Scalability and Implementation Aspects of Cell-Free Massive MIMO for ISAC." In: Proc. IEEE 19th Int. Symp. Wireless Commun. Syst., Jun. 2024, pp. 1-6. doi:10.1109/ISWCS61526.2024.10639146.

128. a, b, cCheng G, Fang Y, Xu J, Ng DWK (2024). "Optimal Coordinated Transmit Beamforming for Networked Integrated Sensing and Communications". IEEE Trans. Wireless Commun.. **23** (8): 8200–8214. doi:10.1109/TWC.2023.3346457.

129. a, bNiu Y, Wei Z, Wang L, Wu H, Feng Z (2024). "Interference Management for Integrated Sensing and Communication Systems: A Survey". IEEE Internet Things J.. doi:10.1109/JIOT.2024.3506162.

130. ^Meng K, Masouros C, Chen G, Liu F (2024). "Network-Level Integrated Sensing and Communication: Interference Management and BS Coordination Using Stochastic Geometry". IEEE Trans. Wireless Commun.. **23** (12): 19365–19381. doi:10.1109/TWC.2024.3483031.

131. a, b, cMasoumi H, Emadi MJ (2020). "Performance Analysis of Cell-Free Massive MIMO System With Limited Fronthaul Capacity and Hardware Impairments." IEEE Trans. Wireless Commun.. **19**(2): 1038-1053. doi:10.1109/TWC.2019.2950316.

132. a, b, cWang D, Wang M, Zhu P, Li J, Wang J, You X (2020). "Performance of Network-Assisted Full-Duplex for Cell-Free Massive MIMO". IEEE Trans. Commun.. **68** (3): 1464-1478.

133. a, bMohammadi M, Mobini Z, Ngo HQ, Matthaiou M (2024). "Ten Years of Research Advances in Full-Duplex Massive MIMO". IEEE Trans. Commun.. doi:10.1109/TCOMM.2024.3464414.

134. ^Zeng F, Yu J, Li J, Liu F, Wang D, You X (2023). "Integrated Sensing and Communication for Network-Assisted Full-Duplex Cell-Free Distributed Massive MIMO Systems". arXiv. Available from: arXiv:2311.05101.

135. ^Zeng F, Liu R, Sun X, Yu J, Li J, Zhu P, Wang D, You X (2024). "Multi-Static ISAC based on Network-Assisted Full-Duplex Cell-Free Networks: Performance Analysis and Duplex Mode Optimization." arXiv. eess.SY. arXiv:2406.08268.

136. ^Zou Q, Behdad Z, Demir ÖT, Cavdar C (2024). "Distributed Versus Centralized Sensing in Cell-Free Massive MIMO". IEEE Wireless Commun. Lett.. doi:10.1109/LWC.2024.3462710.

137. ^Zhou L, Yao J, Jin M, Wu T, Wong K-K (2024). "Fluid antenna-assisted ISAC systems". IEEE Wireless Commun. Lett.. doi:10.1109/LWC.2024.3476148.

138. ^Qin H, Chen W, Wu Q, Zhang Z, Li Z, Cheng N (2024). "Cramér-Rao Bound Minimization for Movable Antenna-Assisted Multiuser Integrated Sensing and Communications." IEEE Wireless Commun. Lett.. doi:10.1109/LWC.2024.3468709.

139. ^Wang C, Li Z, Wong KK, Murch R, Chae CB, Jin S (2024). "AI-Empowered Fluid Antenna Systems: Opportunities, Challenges, and Future Directions." IEEE Wireless Commun.. **31** (5): 34–41. doi:10.1109/MWC.017.2300527.

140. ^Huang C, et al. Holographic MIMO surfaces for 6G wireless networks: Opportunities, challenges, and trends. IEEE Wireless Commun. **27** (5): 118–125, Oct. 2020. doi:10.1109/MWC.001.1900534.

141. ^Adhikary A, Deb Raha A, Qiao Y, Saad W, Han Z, Seon Hong C (2024). "Holographic MIMO with integrated sensing and communication for energy-efficient cell-free 6G networks." IEEE Internet Things J.. **11** (19): 30617–30635. doi:10.1109/JIOT.2024.3411695.

142. ^Zhang J, Miao H, Tang P, Tian L, Liu G (2025). "New mid-band for 6G: Several considerations from the channel propagation characteristics perspective." IEEE Commun. Mag.. **63** (1): 175–180. doi:10.1109/MCOM.001.2300708.

143. ^Chaves F, Chizhik D, Du J, Ghosh A, Love B, Visotsky E (2024). "Coverage evaluation of 7–15 GHz bands from existing sites." Nokia White Paper.

144. ^Zhang H, Shlezinger N, Guidi F, Dardari D, Eldar YC (2023). "6G Wireless Communications: From Far-Field Beam Steering to Near-Field Beam Focusing". IEEE Communications Magazine. **61** (4): 72–77. doi:10.1109/MCOM.001.2200259.

145. a, b Cui M, Wu Z, Lu Y, Wei X, Dai L (2023). "Near-Field MIMO Communications for 6G: Fundamentals, Challenges, Potentials, and Future Directions." IEEE Commun. Mag.. **61** (1): 40–46. doi:10.1109/MCOM.004.2200136.

146. ^Lei H, Zhang J, Wang Z, Ai B, Bjornson E (2025). "Near-field user localization and channel estimation for XL-MIMO systems: Fundamentals, recent advances, and outlooks." IEEE Wireless Commun.. pp. 1–9. doi:10.1109/MWC.010.2400237.

147. ^Bjf6rnson E, Kara F, Kolomvakis N, Kosasih A, Ramezani P, Salman MB (2024). "Enabling 6G performance in the upper mid-band by transitioning from massive to gigantic MIMO". arXiv preprint arXiv:2407.05630. Available from: https://arxiv.org/abs/2407.05630.

148. ^Dong Y, Yang Z, Wang H, Hao N, Li H (2024). "Joint User Pairing and Beamforming Design for NOMA-Aided CFMM-ISAC Systems". IEEE Internet Things J.. doi:10.1109/JIOT.2024.3491137.

149. ^Abdelaziz Salem A, Albreem MA, Alnajjar K, Abdallah S, Saad M (2024). "Integrated Cooperative Sensing and Communication for RIS-Enabled Full-Duplex Cell-Free MIMO Systems". IEEE Trans. Commun.. doi:10.1109/TCOMM.2024.3493795.

150. ^Flores Cabezas XA, da Silva IW, Juntti M. "Performance of UAV-based Cell-free mMIMO ISAC Networks: Tethered vs. Mobile." In: Proc. IEEE Int. Conf. Commun., Jun. 2024, pp. 3549–3554. doi:10.1109/ICC51166.2024.10622699.

151. ^Yu W, Sohrabi F, Jiang T (2022). "Role of Deep Learning in Wireless Communications." IEEE BITS the Info. Theory Mag.. **2** (2): 56–72.

152. ^Hu S, Chen X, Ni W, Hossain E, Wang X (2021). "Distributed Machine Learning for Wireless Communication Networks: Techniques, Architectures, and Applications". IEEE Commun. Surveys Tuts.. **23** (3): 1458–1493.

153. ^Dai L, Jiao R, Adachi F, Poor HV, Hanzo L (2020). "Deep Learning for Wireless Communications: An Emerging Interdisciplinary Paradigm". IEEE Wireless Commun.. **27** (4): 133–139.

154. a, b Demirhan U, Alkhateeb A. "Learning beamforming in cell-free massive MIMO ISAC systems." In: Proc. IEEE Int. Workshop Signal Process. Adv. Wireless Commun.; 2024 Sept. p. 326–330. doi:10.1109/SPAWC60668.2024.10694569.

155. ^Cheng X, Zhang H, Zhang J, Gao S, Li S, Huang Z, Bai L, Yang Z, Zheng X, Yang L (2024). "Intelligent Multi-Modal Sensing-Communication Integration: Synesthesia of Machines". IEEE Commun. Surveys Tuts.. **26** (1): 258–301.

156. ^Liu F, Liu YF, Li A, Masouros C, Eldar YC. "Cram\u00e9r-Rao Bound Optimization for Joint Radar-Communication Beamforming." IEEE Trans Signal Process. **70**:240-253. doi:10.1109/TSP.2021.3135692.

Declarations

Funding: No specific funding was received for this work.

Potential competing interests: No potential competing interests to declare.